A Novel Logarithmic Sine-G Family of Distributions with Applications to Reliability Engineering Data

Zubir Shah[1], Dost Muhammad Khan[1], Amirah Saeed Alharthi[2] and Hassan M. Aljohani[2,*]

[1] Department of Statistics, AbdulWali Khan University, Mardan, Pakistan

[2] Department of Mathematics and Statistics, College of Science, Taif University, Taif, Saudi Arabia

INFORMATION

Keywords:
Logarithmic function
sine function
fundamental properties
estimation
monte carlo simulation study
engineering data modeling

DOI: 10.23967/j.rimni.2026.10.77074

SCIPEDIA Revista Internacional de Métodos Numéricos para Cálculo y Diseño en Ingeniería

Revista Internacional Métodos numéricos para cálculo y diseño en ingeniería RIMNI

In cooperation with CIMNE

A Novel Logarithmic Sine-G Family of Distributions with Applications to Reliability Engineering Data

Zubir Shah[1], **Dost Muhammad Khan**[1], **Amirah Saeed Alharthi**[2] and **Hassan M. Aljohani**[2,*]

[1]Department of Statistics, Abdul Wali Khan University, Mardan, Pakistan

[2]Department of Mathematics and Statistics, College of Science, Taif University, Taif, Saudi Arabia

ABSTRACT

In this research paper, we make a significant attempt to present a novel statistical methodological approach for generating more versatile distributions. The proposed method is developed by incorporating the Logarithmic and Sine functions and may be referred to as a novel logarithmic sine-G (NLS-G) family of distributions. A special sub-model of the NLS-G family is investigated by utilizing the Weibull model as a base member. The sub-model of the NLS-G family may be callednovel logarithmic sine-Weibull (NLS-Weibull) distribution. The density and hazard functions of the NLS-Weibull distribution are graphically illustrated, showing their behavior and characteristics. Some distributional properties of the NLS-G family, including quantile function, median and quartile measures, moments, and moment generating function, are derived. The Maximum Likelihood Estimation (MLE) method is employed for estimating the model parameters of the NLS-G family of distributions. A comprehensive Monte Carlo simulation study of the proposed distribution is also conducted to evaluate the practical performance of its estimators. Furthermore, the usefulness of the newly proposed NLS-Weibull distribution is illustrated by investigating four real data sets from the field of the engineering sector. The first data set represents the failure time of electronic devices. The second data set is civil engineering data and represents the breaking stress of carbon fibers. The third data set represents the strengths of 1.5 cm glass fibers. The fourth data set represents single-carbon fibers. Based on four diagnostic criteria, it is observed that the NLS-Weibull distribution may be the best choice for the considered data sets.

OPEN ACCESS

Received: 02/12/2025

Accepted: 12/01/2026

Published: 29/05/2026

DOI
10.23967/j.rimni.2026.10.77074

Keywords:
Logarithmic function
sine function
fundamental properties
estimation
monte carlo simulation study
engineering data modeling

1 Introduction

In the literature of distribution theory, various probability distributions have been introduced for predicting and analyzing real-world phenomena in different applied sectors, such as the engineering sector, education, healthcare and biomedical sectors, actuarial and management sciences, and hydrology. But still, no particular probability distribution is proposed to handle every phenomenon

*Correspondence: Hassan M. Aljohani (hmjohani@tu.edu.sa).

because real-world phenomena are complex. Therefore, the researchers are constantly struggling to propose new families of probability distributions with greater distributional flexibility. Most of the new families of probability distributions are proposed with the help of adding additional parameters to the existing distributions, ranging from one to seven; for further details, see Almalki and Yuan (2013) [1]. In this context, the following are some notable families of distributions that have been proposed in the literature of distribution theory: An exponentiated family of distributions proposed by Mudholkar and Srivastava (1993) [2]. They used the Weibull distribution as a baseline distribution and proposed a new distribution called the exponentiated Weibull distribution. Using the exponentiated method, various distributions are generalized, such as Nadarajah and Kotz (2003) [3] used the exponentiated method and proposed the exponentiated Fréchet distribution. Nadarajah (2011) [4] proposed the exponentiated exponential distribution. Salem (2014) [5] developed the exponentiated Lomax distribution. Ashour and Eltehiwy (2015) [6] proposed the exponentiated power Lindley distribution and many more.

Marshal and Olkin (1997) [7] proposed another method to generate new distributions. They named their proposed method the Marshal Olkin family of probability distributions. Using the Marshal and Olkin family, several existing distributions are modified: the Marshal Olkin Weibull distribution proposed by Ghitany et al. (2005) [8], the Marshal Olkin Lomax distribution proposed by Ghitany et al. (2007) [9], the Marshal Olkin Fréchet distribution proposed by Krishna et al. (2013) [10], and the Marshal Olkin Burr XII distribution proposed by Al-Saiari et al. (2014) [11]. Furthermore, in the past decade, Mahdavi and Kundu (2017) [12] proposed the Alpha Power Transformations family of distributions with application to the exponential distribution, using extra parameters to bring more flexibility to the generated distributions. Using the Alpha Power Transformation family, several distributions have been suggested in the literature on distributions theory: Alpha Power Transformed Weibull distribution suggested by Dey et al. (2017) [13], Alpha Power Transformed Pareto distribution suggested by Ihtisham et al. (2019) [14], Alpha Power Transformed Lindley distribution suggested by Dey et al. (2019) [15], Alpha Power Transformed Lomax distribution suggested by Amer (2020) [16], and Alpha Power Transformed Inverse Lomax distribution suggested by ZeinEldin et al. (2020) [17]. For more details about the introduced families of probability distributions, please see the references, Bakr et al. (2022) [18], Alsadat et al. (2023) [19], Shah et al. (2025) [20], Osi et al. (2025) [21], Hassan et al. (2025) [22], and Alsolmi (2025) [23].

Recently, Zhao et al. (2023) [24] have developed a Novel Logarithmic family (NL-F) of distributions with application to the Weibull distribution, using two additional parameters to make the generated distribution more flexible. The cumulative distribution function (CDF) $F(t;\beta,\phi,\vartheta)$ of the NL-F is given by

$$F(t;\beta,\phi,\vartheta) = 1 - \left[1 - \frac{\beta G(t;\vartheta)}{\beta - (\log G(t;\vartheta))}\right]^{\phi} \beta,\phi \in \Re^{+}, t \in \Re. \tag{1}$$

Shah et al. (2023) [25] have suggested a New Generalized Logarithmic-X (NGL-X) family of distributions by adding one additional parameter with fundamental properties and application to the baseline Weibull distribution. They used a well-known T-X family method (developed by Alzaatreh et al. (2013) [26]) and derived the suggested family of distributions. The following is the CDF $F(t;\phi,\vartheta)$ of the NGL-X family

$$F(t;\phi,\vartheta) = \frac{e^{\phi} G(t;\vartheta)}{[e - \log(G(t;\vartheta))]^{\phi}} \quad t \in \Re, \tag{2}$$

where, $\phi \in \Re^+$ (additional shape parameter), and $G(t;\vartheta)$ is the CDF of any baseline distributions depending on the parameter vector ϑ.

Similarly, Kamal et al. (2023) [27] have incorporated a trigonometric function and developed another method called the New Trigonometric Sine-G (NTS-G) family of distributions. The CDF $F(t;\phi,\vartheta)$ of their developed family of distributions is given by

$$F(t;\phi,\vartheta) = 1 - \frac{\phi\left[1-\sin\left(\frac{\pi}{2}G(t;\vartheta)\right)\right]}{\phi-\sin\left(\frac{\pi}{2}G(t;\vartheta)\right)} \quad t \in \Re, \tag{3}$$

where, $\phi \in \Re^+$ additional parameter and $G(t;\vartheta)$ is the CDF of any baseline (or classical) distributions depending on the parameter vector ϑ.

Taking motivation from the above brief discussion, we are also proposing a new family of distributions. The proposed method is derived based on logarithmic and sine functions. The proposed method is called a Novel Logarithmic Sine-G family of distributions. In the very next section, with the help of the Novel Logarithmic Sine-G (NLS-G) family, we proposed the updated version of the Weibull distribution. The updated version is called a Novel Logarithmic Sine Weibull distribution. In Section 3, some fundamental properties of the proposed family are derived. In Section 4, the Maximum Likelihood estimation method is used to estimate the model parameters of the suggested family. In Section 5, a comprehensive simulation analysis is conducted to evaluate the behavior of the estimators of the proposed work. In Section 6, four real data sets from the engineering sector are used for compression purposes. The comparison is made with other well-known distributions in the literature. Finally, some concluding remarks are presented in Section 7.

Definition 1: *Let $G(t;\vartheta)$ be the CDF of any baseline distributions having the PDF (probability density function) $g(t;\vartheta)$ and SF (survival function) $S(t;\vartheta)$; that are $g(t;\vartheta) = \frac{d}{dt}G(t;\vartheta)$ and $S(t;\vartheta) = 1 - G(t;\vartheta)$. Then the CDF $F(t;\phi,\vartheta)$ of the new logarithmic sine-G family of probability distributions is given by*

$$F(t;\phi,\vartheta) = 1 - \frac{\log\left[e^{\phi} + \left(1 - e^{\phi\sin\left(\frac{\pi}{2}G(t;\vartheta)\right)}\right)\right]}{\phi} \quad \phi \in \Re^+, \quad t \in \Re, \tag{4}$$

where, $\phi \in \Re^+$ is an extra shape parameter and $G(t;\vartheta)$ is the CDF of any baseline distributions, which depends on a vector parameter $\vartheta \in \Re$. To verify whether the CDF $F(t;\phi,\vartheta)$ is a real CDF or not. For this purpose, we have the following two propositions.

Proposition 1: *For Eq. (4), we need to prove*

$\lim_{x\to-\infty} F(t;\phi,\vartheta) = 0$, and $\lim_{x\to\infty} F(t;\phi,\vartheta) = 1$.

Proof: From Eq. (4), we have

$$\lim_{x\to-\infty} F(t;\phi,\vartheta) = 1 - \frac{\log\left[e^{\phi} + \left(1 - e^{\phi\sin\left(\frac{\pi}{2}G(-\infty;\vartheta)\right)}\right)\right]}{\phi}, \tag{5}$$

where, $G(t;\vartheta)$ is a valid CDF of any base models. So, we have

$\lim_{x\to-\infty} G(t;\vartheta) = G(-\infty;\vartheta) = 0$ and $\mathrm{Sin}(0) = 0$.

Now, from Eq. (5), we have

$$\lim_{x\to-\infty} F(t;\phi,\vartheta) = 1 - \frac{\log\left[e^{\phi} + \left(1 - e^{0}\right)\right]}{\phi},$$

$\lim_{x\to-\infty} F(t;\phi,\vartheta) = 0.$

Again, applying the limit of Eq. (4), we have

$$\lim_{x\to\infty} F(t;\phi,\vartheta) = 1 - \frac{\log\left[e^{\phi} + \left(1 - e^{\phi \sin\left(\frac{\pi}{2}G(\infty;\vartheta)\right)}\right)\right]}{\phi}. \tag{6}$$

As we have mentioned that $G(t;\vartheta)$ is a valid CDF of any base distributions. So, we have $\lim_{x\to\infty} G(t;\vartheta) = G(\infty;\vartheta) = 1$ and $\text{Sin}\left(\frac{\pi}{2}\right) = 1$.

Now, from Eq. (6), we have

$$\lim_{x\to\infty} F(t;\phi,\vartheta) = 1 - \frac{\log\left[e^{\phi} + (1 - e^{\phi})\right]}{\phi},$$

$\lim_{x\to\infty} F(t;\phi,\vartheta) = 1$. □

Proposition 2: *The CDF $F(t;\phi,\vartheta)$ is right continuous (non-negative) and differentiable.*

Proof: $\frac{d}{dt}F(t;\phi,\vartheta) = f(t;\phi,\vartheta)$.

Henceforth, from Propositions 1 and 2, it is clearly observed that the expression in Eq. (4) is an actual CDF and very attractive. The PDF $f(t;\phi,\vartheta)$ corresponding to Eq. (4) is given by

$$f(t;\phi,\vartheta) = \frac{\pi g(t;\vartheta)\cos\left(\frac{\pi}{2}G(t;\vartheta)\right)e^{\phi \sin\left(\frac{\pi}{2}G(t;\vartheta)\right)}}{2\left[e^{\phi} + \left(1 - e^{\phi \sin\left(\frac{\pi}{2}G(t;\vartheta)\right)}\right)\right]} \quad t \in \Re. \tag{7}$$

Furthermore, the SF $S(t;\phi,\vartheta) = 1 - F(t;\phi,\vartheta)$, HF $h(t;\phi,\vartheta) = \frac{f(t;\phi,\vartheta)}{S(t;\phi,\vartheta)}$, reverse HF (RHF) $\tau(t;\phi,\vartheta) = \frac{f(t;\phi,\vartheta)}{F(t;\phi,\vartheta)}$, and the corresponding CHF (cumulative HF) $H(t;\phi,\vartheta) = -\log\left(S(t;\phi,\vartheta)\right)$ of the NLS-G family, corresponding to Eq. (4), are the following

$$S(t;\phi,\vartheta) = \frac{\log\left[e^{\phi} + \left(1 - e^{\phi \sin\left(\frac{\pi}{2}G(t;\vartheta)\right)}\right)\right]}{\phi} \quad t \in \Re,$$

$$h(t;\phi,\vartheta) = \frac{\pi\phi g(t;\vartheta)\cos\left(\frac{\pi}{2}G(t;\vartheta)\right)e^{\phi \sin\left(\frac{\pi}{2}G(t;\vartheta)\right)}}{2\log\left[e^{\phi} + \left(1 - e^{\phi \sin\left(\frac{\pi}{2}G(t;\vartheta)\right)}\right)\right]\left[e^{\phi} + \left(1 - e^{\phi \sin\left(\frac{\pi}{2}G(t;\vartheta)\right)}\right)\right]} \quad t \in \Re,$$

$$\tau(t;\phi,\vartheta) = \frac{\pi\phi g(t;\vartheta)\cos\left(\frac{\pi}{2}G(t;\vartheta)\right)e^{\phi \sin\left(\frac{\pi}{2}G(t;\vartheta)\right)}}{2\left\{\phi - \log\left[e^{\phi} + \left(1 - e^{\phi \sin\left(\frac{\pi}{2}G(t;\vartheta)\right)}\right)\right]\right\}\left[e^{\phi} + \left(1 - e^{\phi \sin\left(\frac{\pi}{2}G(t;\vartheta)\right)}\right)\right]} \quad t \in \Re,$$

and

$$H(t;\phi,\vartheta) = -\log\left\{\frac{\log\left[e^{\phi} + \left(1 - e^{\phi \sin\left(\frac{\pi}{2}G(t;\varpi)\right)}\right)\right]}{\phi}\right\} \quad t \in \Re. \square$$

2 NLS-Weibull Distribution

Hew, we set the classical Weibull distribution in the proposed method and derived a special model of the proposed family. This special model (or distribution) is called the new logarithmic sine Weibull (NLS-Weibull for short) distribution. If a random variable $T\ (\in \Re^+)$ follow the CDF $G\left(t;\vartheta\right)=1-e^{-\delta t^{\theta}}$ and PDF $g\left(t;\vartheta\right)=\delta\theta t^{\theta-1}e^{-\delta t^{\theta}}$ of the Weibull distribution with parameters $\delta>0$ and $\theta>0$, then the CDF $F\left(t;\phi,\vartheta\right)$ and SF $S\left(t;\phi,\vartheta\right)$ of the NLS-Weibull distribution is given by

$$F\left(t;\phi,\vartheta\right)=1-\frac{\log\left[e^{\phi}+\left(1-e^{\phi\sin\left[\frac{\pi}{2}\left(1-e^{-\delta t^{\theta}}\right)\right]}\right)\right]}{\phi}\quad t\in\Re^+. \tag{8}$$

Some graphical representation of the CDF $F\left(t;\phi,\vartheta\right)$ of the NLS-Weibull distribution are sketched in Fig. 1. The plots are obtained for (i) $\phi=0.2$, $\delta=0.2$, $\theta=4.6$ (red-line), (ii) $\phi=0.1$, $\delta=0.5$, $\theta=1.7$ (green-line), and (iii) $\phi=0.09$, $\delta=0.02$, $\theta=5.2$ (blue-line).

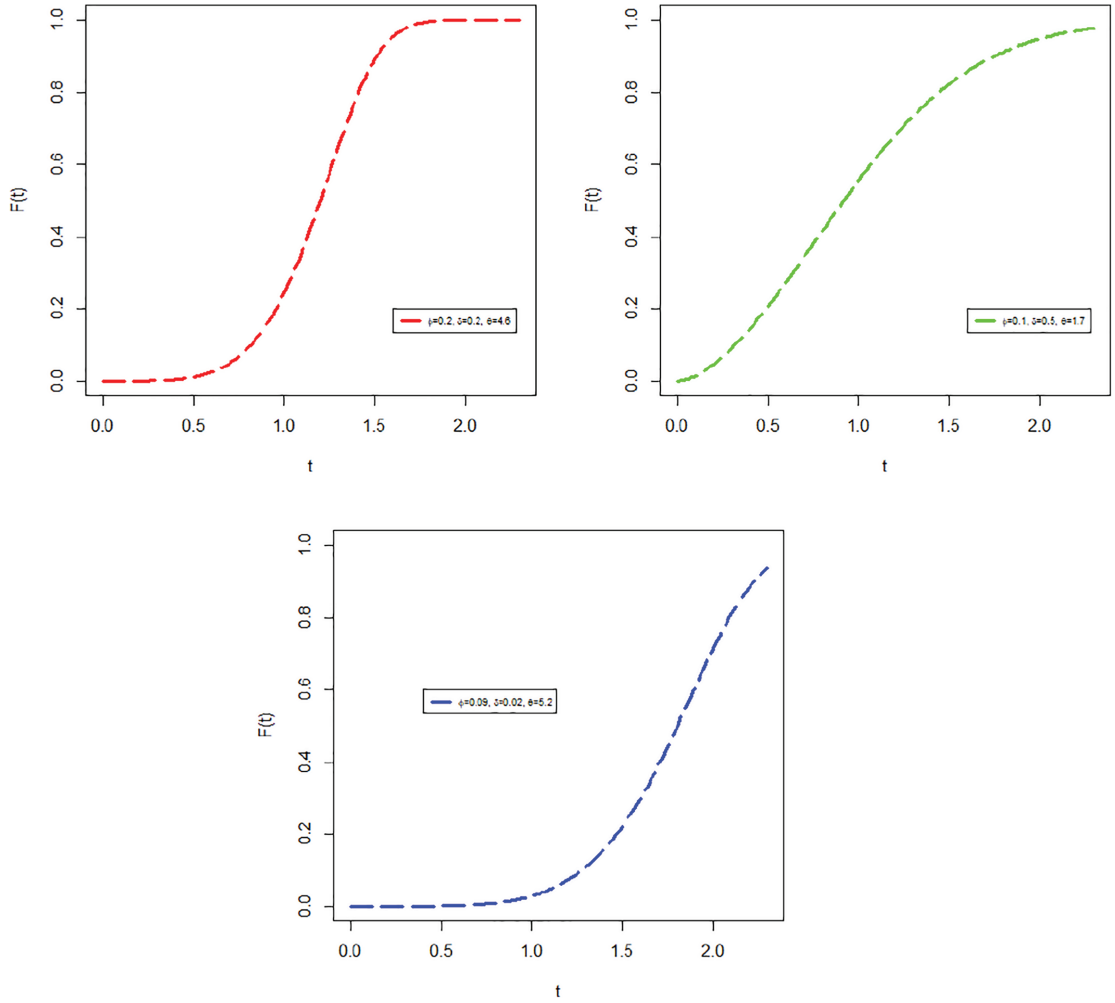

Figure 1: Plots of CDF $F\left(t;\phi,\vartheta\right)$ of the NLS-Weibull distribution

Corresponding to Eq. (8), the SF of the NLS-Weibull distribution is given by

$$S(t;\phi,\vartheta) = \frac{\log\left[e^{\phi} + \left(1 - e^{\phi \sin\left[\frac{\pi}{2}\left(1-e^{-\delta t^{\theta}}\right)\right]}\right)\right]}{\phi} \quad t \in \Re^{+}. \tag{9}$$

Similarly, some graphical representation of the SF $S(t;\phi,\vartheta)$ of the NLS-Weibull distribution are sketched in Fig. 2. These plots are also obtained for (i) $\phi = 0.2$, $\delta = 0.2$, $\theta = 4.6$ (red-line), (ii) $\phi = 0.1$, $\delta = 0.5$, $\theta = 1.7$ (green-line), and (iii) $\phi = 0.09$, $\delta = 0.02$, $\theta = 5.2$ (blue-line).

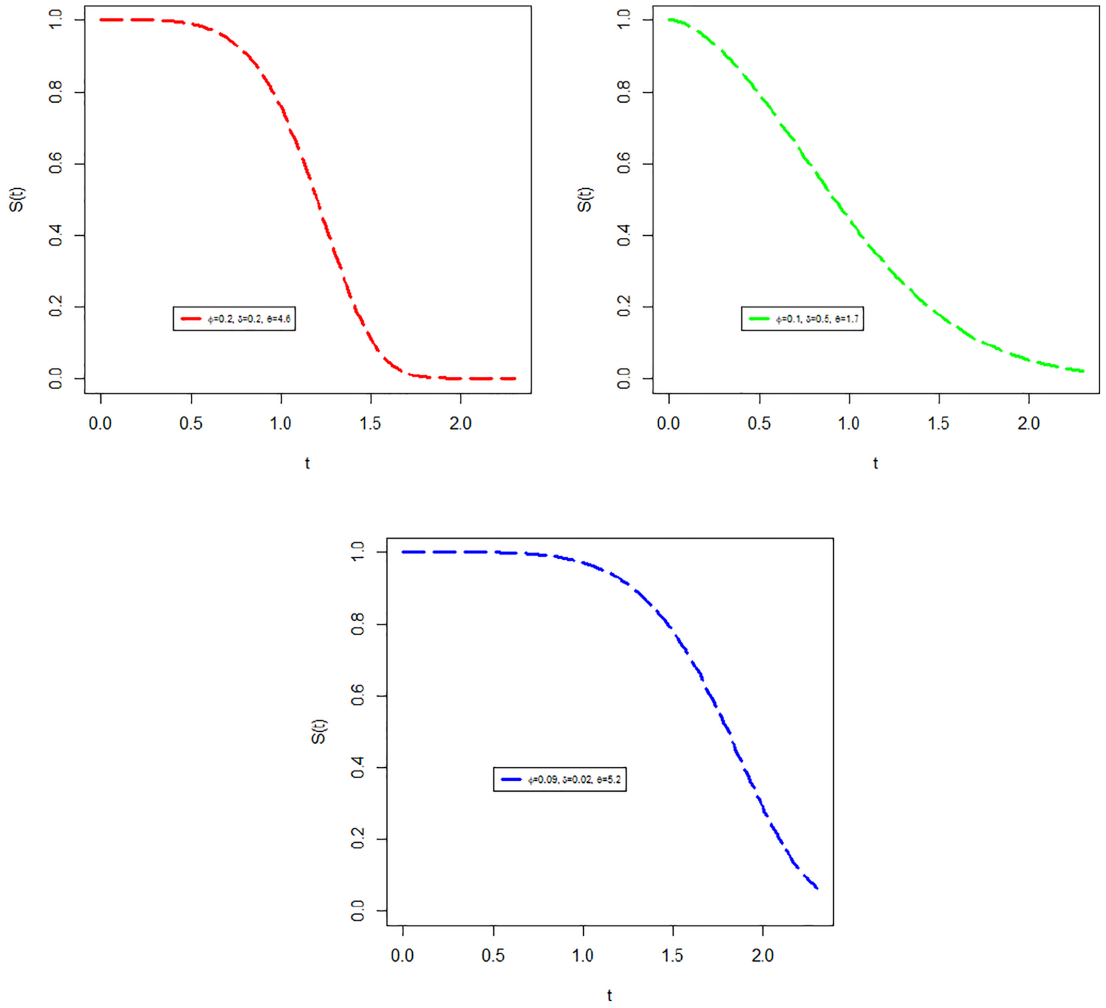

Figure 2: Plots of SF $S(t;\phi,\vartheta)$ of the NLS-Weibull distribution

In link to Eqs. (8) and (9), the PDF $f(t;\phi,\vartheta)$, and HF $h(t;\phi,\vartheta)$ of the NLS-Weibull distribution are respectively given by

$$f(t;\phi,\vartheta) = \frac{\pi\delta\theta t^{\theta-1}e^{-\delta t^{\theta}}\cos\left[\frac{\pi}{2}\left(1-e^{-\delta t^{\theta}}\right)\right]e^{\phi\sin\left[\frac{\pi}{2}\left(1-e^{-\delta t^{\theta}}\right)\right]}}{2\left[e^{\phi} + \left(1 - e^{\phi\sin\left[\frac{\pi}{2}\left(1-e^{-\delta t^{\theta}}\right)\right]}\right)\right]} \quad t \in \Re^{+}, \tag{10}$$

$$h\left(t;\phi,\vartheta\right)=\frac{\pi\phi\delta\theta t^{\theta-1}e^{-\delta t^{\theta}}\cos\left[\frac{\pi}{2}\left(1-e^{-\delta t^{\theta}}\right)\right]e^{\phi\sin\left[\frac{\pi}{2}\left(1-e^{-\delta t^{\theta}}\right)\right]}}{2\log\left[e^{\phi}+\left(1-e^{\phi\sin\left[\frac{\pi}{2}\left(1-e^{-\delta t^{\theta}}\right)\right]}\right)\right]\left[e^{\phi}+\left(1-e^{\phi\sin\left[\frac{\pi}{2}\left(1-e^{-\delta t^{\theta}}\right)\right]}\right)\right]}\quad t\in\Re^{+}. \tag{11}$$

For visual illustration, some basic plots for PDF $f\left(t;\phi,\vartheta\right)$ ad HF $h\left(t;\phi,\vartheta\right)$ of the NLS-Weibull distribution are sketched in Fig. 3. The plots of the PDF $f\left(t;\phi,\vartheta\right)$ are displayed with different parameter values such as (i) $\phi=0.1$, $\delta=0.1$, $\theta=5.2$ (violet line), (ii) $\phi=0.2$, $\delta=0.5$, $\theta=3.6$ (green line), (iii) $\phi=0.2$, $\delta=1.3$, $\theta=2.8$ (black line), (iv) $\phi=0.9$, $\delta=0.05$, $\theta=5.6$ (blue line), and (iv) $\phi=0.1$, $\delta=2.3$, $\theta=1.9$ (red line). From the Fig. 3 lift penal plot, we can see that the $f\left(t;\phi,\vartheta\right)$ shape of the NLS-Weibull distribution can exhibit different behaviors, such as (i) left skewed, (ii) symmetrical, and (iii) right skewed.

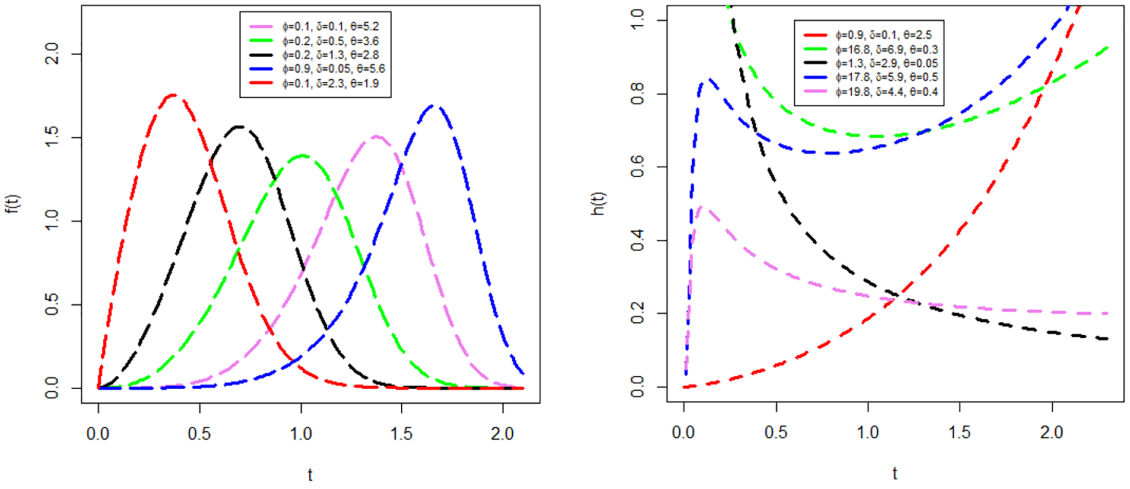

Figure 3: The plots of $f\left(t;\phi,\vartheta\right)$ and $h\left(t;\phi,\vartheta\right)$ of the NLS-Weibull distribution

Similarly, the plots of HF $h\left(t;\phi,\vartheta\right)$ of the NLS-Weibull distribution are obtained with different combinations of the parameter values, such as (i) $\phi=0.9$, $\delta=0.1$, $\theta=2.5$ (red line), (ii) $\phi=16.8$, $\delta=6.9$, $\theta=0.3$ (green line), (iii) $\phi=1.3$, $\delta=2.9$, $\theta=0.05$ (black line), (iv) $\phi=17.8$, $\delta=5.9$, $\theta=0.5$ (blue line), and (iv) $\phi=19.8$, $\delta=4.4$, $\theta=0.4$ (violet line). Similarly, from the right panel of Fig. 3, we can also see that the $h\left(t;\phi,\vartheta\right)$ shape of the NLS-Weibull distribution can exhibit different behaviors such as increasing, decreasing, unimodal, increasing-decreasing-increasing, and bathtub patterns.

Furthermore, in linked to the Eqs. (8)–(10), the RHF $H\left(t;\phi,\vartheta\right)$ and CHF $\tau\left(t;\phi,\vartheta\right)$ of the NLS-Weibull distribution are given, respectively, by

$$\tau\left(t;\phi,\vartheta\right)=\frac{\pi\phi\delta\theta t^{\theta-1}e^{-\delta t^{\theta}}\cos\left[\frac{\pi}{2}\left(1-e^{-\delta t^{\theta}}\right)\right]e^{\phi\sin\left[\frac{\pi}{2}\left(1-e^{-\delta t^{\theta}}\right)\right]}}{2\left\{\phi-\log\left[e^{\phi}+\left(1-e^{\phi\sin\left[\frac{\pi}{2}\left(1-e^{-\delta t^{\theta}}\right)\right]}\right)\right]\right\}\left[e^{\phi}+\left(1-e^{\phi\sin\left[\frac{\pi}{2}\left(1-e^{-\delta t^{\theta}}\right)\right]}\right)\right]}\quad t\in\Re^{+},$$

and

$$H\left(t;\phi,\vartheta\right)=-\log\left\{1-\frac{\log\left[e^{\phi}+\left(1-e^{\phi\sin\left[\frac{\pi}{2}\left(1-e^{-\delta t^{\theta}}\right)\right]}\right)\right]}{\phi}\right\}\quad t\in\Re^{+}.$$

3 Fundamental Properties

Here in the present section, we discuss some distributional (or statistical) properties of the NLS-G family of distributions. These properties are based on the quantile function, median and quartiles measures, skewness, kurtosis, rth moments, and moment generating functions. The motivations of these properties of the distribution are used to study the characteristics and nature of the distribution. For example, the skewness of the distribution studies the nature of the distribution, such as symmetry and asymmetry. Similarly, the measure of kurtosis is used to study the peakedness of the distribution, such as platykurtic, mesokurtic, and leptokurtic of distributions.

3.1 Quantile Function

If T follows the NLS-G family of distributions, then the quartile function (QF), say $Q(u)$, is given by

$$Q(u) = G^{-1}\left\{\frac{2}{\pi}\sin^{-1}\left[\frac{\log\left(1-e^{\phi(1-u)}+e^{\phi}\right)}{\phi}\right]\right\}, \tag{12}$$

where, $0 < u < 1$.

Eq. (12) shows the explicit form of the quantile function of the NLS-G family, which helps to generate the random numbers easily.

3.2 Median and Quartile Measures

In this sub-section, we discuss the median (which is also known is the second quartile) and other quartile measures of the NLS-G family of distributions. Let T follow the NLS-G family of distributions, then the Median, say $Q\left(\frac{1}{2}\right)$, is given by

$$Q\left(\frac{1}{2}\right) = G^{-1}\left\{\frac{2}{\pi}\sin^{-1}\left[\frac{\log\left(1-e^{\frac{1}{2}\phi}+e^{\phi}\right)}{\phi}\right]\right\}.$$

Furthermore, the 1st and 3rd quartiles of the NLS-G family of distribution are derived by replacing $u = \frac{1}{4}$ and $u = \frac{3}{4}$ in Eq. (12). Henceforward, the 1st and 3rd quartiles of the proposed family of distributions are given, respectively, by

$$Q\left(\frac{1}{4}\right) = G^{-1}\left\{\frac{2}{\pi}\sin^{-1}\left[\frac{\log\left(1-e^{\frac{3}{4}\phi}+e^{\phi}\right)}{\phi}\right]\right\}.$$
$$Q\left(\frac{3}{4}\right) = G^{-1}\left\{\frac{2}{\pi}\sin^{-1}\left[\frac{\log\left(1-e^{\frac{1}{4}\phi}+e^{\phi}\right)}{\phi}\right]\right\}.$$

The GSK (Galton skewness) of the NLS-G family of distribution, say $GSK(t)$, is given by

$$GSK(t) = \frac{Q\left(\frac{6}{8}\right) - 2Q\left(\frac{4}{8}\right) + Q\left(\frac{2}{8}\right)}{Q\left(\frac{6}{8}\right) - Q\left(\frac{2}{8}\right)},$$

where, the quantities $Q\left(\frac{2}{8}\right)$, $Q\left(\frac{4}{8}\right)$, and $Q\left(\frac{6}{8}\right)$ are obtained by replacing $u=\frac{2}{8}$, $u=\frac{4}{8}$, and $u=\frac{6}{8}$ respectively in Eq. (12).

Similarly, the MKU (Moors kurtosis) of the NLS-G family of distribution, say $MKU\,(t)$, is given by

$$MKU\,(t)=\frac{Q\left(\frac{7}{8}\right)-Q\left(\frac{5}{8}\right)-Q\left(\frac{1}{8}\right)+Q\left(\frac{3}{8}\right)}{Q\left(\frac{6}{8}\right)-Q\left(\frac{2}{8}\right)},$$

where, the quantities $Q\left(\frac{1}{8}\right)$, $Q\left(\frac{2}{8}\right)$, $Q\left(\frac{3}{8}\right)$, $Q\left(\frac{5}{8}\right)$, $Q\left(\frac{6}{8}\right)$ and $Q\left(\frac{7}{8}\right)$ are obtained by replacing $u=\frac{1}{8}, \frac{2}{8}, \frac{3}{8}, \frac{5}{8}, \frac{6}{8}$, and $u=\frac{7}{8}$ respectively in Eq. (12).

3.3 Moments

If a random variable T follow the NLS-G family of distribution with PDF $f\,(t;\phi,\vartheta)$, then the r^{th} moments, say μ', is derived as

$$\mu'=E\,(t^r)=\int_{-\infty}^{\infty}t^r f\,(t;\phi,\vartheta)\,dt. \tag{13}$$

Now, putting the PDF $f\,(t;\phi,\vartheta)$ of the NLS-G family of distributions in Eq. (13), then we obtain

$$\mu'=E\,(t^r)=\int_{-\infty}^{\infty}t^r\frac{\pi g\,(t;\vartheta)\cos\left(\frac{\pi}{2}G\,(t;\vartheta)\right)e^{\phi\sin\left(\frac{\pi}{2}G(t;\vartheta)\right)}}{2\left[e^{\phi}+\left(1-e^{\phi\sin\left(\frac{\pi}{2}G(t;\vartheta)\right)}\right)\right]}dt,$$

$$\mu'=\int_{-\infty}^{\infty}t^r\frac{\pi}{2}e^{\phi}g\,(t;\vartheta)\cos\left(\frac{\pi}{2}G\,(t;\vartheta)\right)e^{\phi\sin\left(\frac{\pi}{2}G(t;\vartheta)\right)}\left[1+e^{-\phi}\left(1-e^{\phi\sin\left(\frac{\pi}{2}G(t;\vartheta)\right)}\right)\right]^{-1}dt. \tag{14}$$

Appling some algebraic expansion

$$(1+t)^{-1}=\sum_{i=0}^{\infty}(-1)^i t^i \quad -\infty<t<\infty,$$

$$(1-t)^i=\sum_{j=0}^{i}(-1)^j\binom{i}{j}t^j \quad |t|<1,$$

$$e^t=\sum_{k=1}^{\infty}\frac{t^k}{k!} \quad -\infty<t<\infty.$$

Using these algebraic expansions in Eq. (14), the moments can be expressed as a linear as

$$\mu'=\frac{\pi}{2}\sum_{i=0}^{\infty}\sum_{j=0}^{i}\sum_{k=1}^{\infty}\frac{e^{(1-i)\phi}(-1)^{i+j}(1+j)^k\phi^k}{k!}\binom{i}{j}\psi_{r,i,j,k}\,(t;\vartheta),$$

where, $\psi_{r,i,j,k}\,(t;\vartheta)=\int_{-\infty}^{\infty}t^r g\,(t;\vartheta)\cos\left(\frac{\pi}{2}G\,(t;\vartheta)\right)\left(\sin\left(\frac{\pi}{2}G\,(t;\vartheta)\right)\right)^k dt.$

For different values of parameters, the graphical illustrations of the mean, variance, skewness, and kurtosis of the proposed distribution are visualized in Figs. 4 and 5.

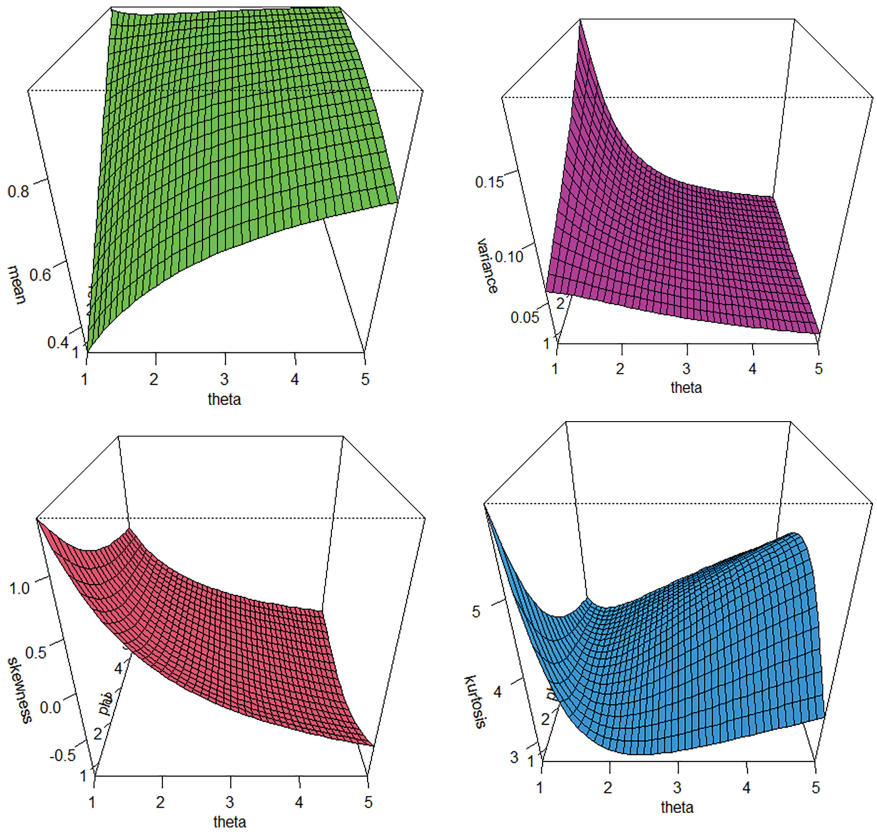

Figure 4: The graphical illustration of the mean, variance, skewness, and kurtosis of the NLS-Weibull distribution with different parameter values

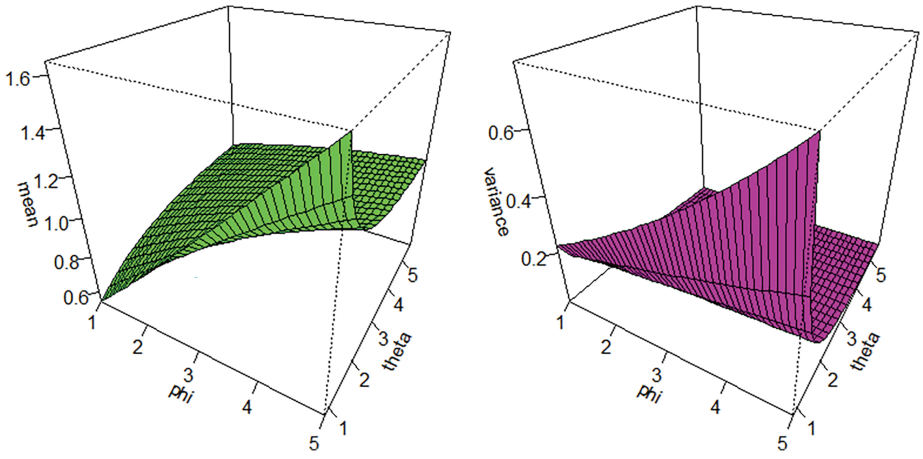

Figure 5: (Continued)

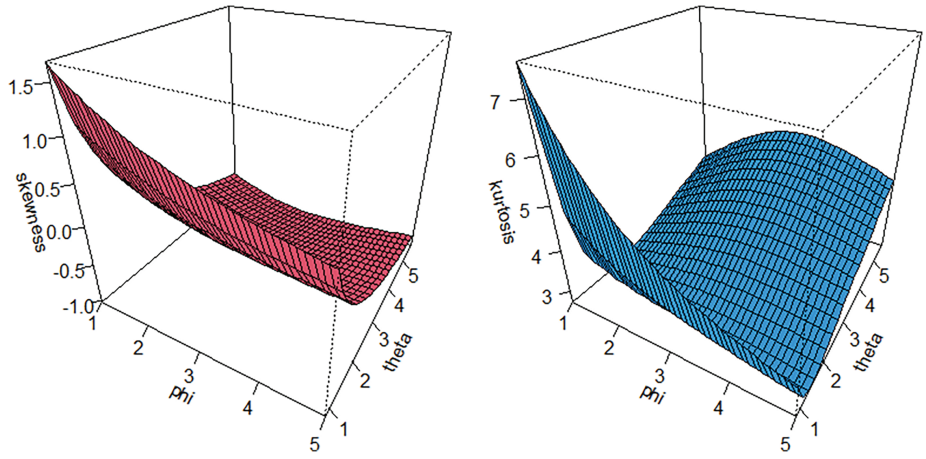

Figure 5: The graphical illustrations of the mean, variance, skewness, and kurtosis of the NLS-Weibull distribution with different parameter values

Furthermore, the MGF (moment generating function), say $M_t(x)$, of the NLS-G family of distributions is derived as

$$M_t(x) = \int_{-\infty}^{\infty} e^{xt} f(t;\phi,\vartheta)\, dt. \tag{15}$$

Using the series $e^t = \sum_{r=0}^{\infty} \frac{t^r}{r!}$, and after simplification, we get

$$M_t(x) = \sum_{r=0}^{\infty} \frac{x^r}{r!} \int_{-\infty}^{\infty} t^r f(t;\phi,\vartheta)\, dt,$$
$$M_t(x) = \frac{\pi}{2} \sum_{r=0}^{\infty} \sum_{i=0}^{\infty} \sum_{j=0}^{i} \sum_{k=1}^{\infty} \frac{x^r e^{(1-i)\phi} (-1)^{i+j} (1+j)^k \phi^k}{k!\, r!} \binom{i}{j} \psi_{r,i,j,k}(t;\vartheta). \tag{16}$$

4 Maximum Likelihood Function

In the present section, we use the well-known method of maximum Likelihood estimation (MLE) to estimate the model parameters, i.e., MLEs $\left(\hat{\phi}_{MLE}, \hat{\vartheta}_{MLE}\right)$ of the parameters (ϕ,ϑ) of the NLS-G family of distribution. Let $T_1, T_2, T_3, \ldots, T_n$ are the random sample of size n taken from the NLS-G family with PDF $f(t;\phi,\vartheta)$, then the LHF (likelihood-function) corresponding to the PDF is given by

$$\Upsilon(t;\phi,\vartheta) = \prod_{i=1}^{c} f(t;\phi,\vartheta). \tag{17}$$

Using PDF $f(t;\phi,\vartheta)$ in Eq. (17), we get

$$\Upsilon(t;\phi,\vartheta) = \prod_{i=1}^{n} \frac{\pi g(t;\vartheta) \cos\left(\frac{\pi}{2} G(t;\vartheta)\right) e^{\phi \sin\left(\frac{\pi}{2} G(t;\vartheta)\right)}}{2\left[e^{\phi} + \left(1 - e^{\phi \sin\left(\frac{\pi}{2} G(t;\vartheta)\right)}\right)\right]},$$

The LLHF (log LHF), say $\ell(\phi, \vartheta)$, is given by

$$\ell(\phi,\vartheta) = n\log\pi - n\log 2 + \sum_{i=1}^{n}\log g(t_i;\vartheta) + \sum_{i=1}^{n}\log\cos\left(\tfrac{\pi}{2}G(t_i;\vartheta)\right) + \phi\sum_{i=1}^{n}\sin\left(\tfrac{\pi}{2}G(t_i;\vartheta)\right) - \sum_{i=1}^{n}\log\left[e^{\phi} + \left(1 - e^{\phi\sin\left(\frac{\pi}{2}G(t_i;\vartheta)\right)}\right)\right]. \tag{18}$$

Corresponding to Eq. (18), the partial derivatives based on ϕ and ϑ, are given by

$$\frac{\partial}{\partial\phi}\ell(\phi,\vartheta) = \sum_{i=1}^{n}\sin\left(\frac{\pi}{2}G(t_i;\vartheta)\right) - \sum_{i=1}^{n}\frac{\partial\left[e^{\phi} + \left(1 - e^{\phi\sin\left(\frac{\pi}{2}G(t_i;\vartheta)\right)}\right)\right]/\partial\phi}{\left[e^{\phi} + \left(1 - e^{\phi\sin\left(\frac{\pi}{2}G(t_i;\vartheta)\right)}\right)\right]},$$

and

$$\frac{\partial}{\partial\vartheta}\ell(\phi,\vartheta) = \sum_{i=1}^{n}\frac{\partial g(t_i;\vartheta)/\partial\vartheta}{g(t_i;\vartheta)} - \sum_{i=1}^{n}\frac{\pi}{2}\frac{\sin\left(\frac{\pi}{2}G(t_i;\vartheta)\right)\partial G(t_i;\vartheta)/\partial\vartheta}{\cos\left(\frac{\pi}{2}G(t_i;\vartheta)\right)} + \phi\sum_{i=1}^{n}\frac{\pi}{2}\frac{\cos\left(\frac{\pi}{2}G(t_i;\vartheta)\right)\partial G(t_i;\vartheta)/\partial\vartheta}{\sin\left(\frac{\pi}{2}G(t_i;\vartheta)\right)} - \sum_{i=1}^{n}\frac{\partial\left[e^{\phi} + \left(1 - e^{\phi\sin\left(\frac{\pi}{2}G(t_i;\vartheta)\right)}\right)\right]/\partial\vartheta}{\left[e^{\phi} + \left(1 - e^{\phi\sin\left(\frac{\pi}{2}G(t_i;\vartheta)\right)}\right)\right]}.$$

Solving numerically $\frac{\partial}{\partial\phi}\ell(\phi,\vartheta) = 0$ and $\frac{\partial}{\partial\vartheta}\ell(\phi,\vartheta) = 0$ simultaneously, we get MLEs $\left(\hat{\phi},\hat{\vartheta}\right)$ of (ϕ,ϑ).

5 Simulations

This section of the article is based on the evaluation of the applied estimation approach for the newly proposed NLS-Weibull distribution. A Monte Carlo Simulation study (MCSS) is conducted to check the effectiveness of the MLE approach for the NLS-Weibull distribution. The inverse of the CDF of the NLS-Weibull distribution is employed to generate random numbers (RANs) from the NLS-Weibull distribution. The MCSS is carried out for four different sets of the initial values of the parameter, such as Set I: $\phi = 2.7, \delta = 3.7, \theta = 1.5$, Set II: $\phi = 1.7, \delta = 2.9, \theta = 0.6$, Set III: $\phi = 1.5$, $\delta = 3.7$, $\theta = 1.0$, and Set IV: $\phi = 4.9$, $\delta = 0.6$, $\theta = 2.4$. The MCSS involved sample sizes of 25, 50, 75, 100, 200, 300, 400, 500, 600, 700, 800, 900, and 1000. Each procedure is simulated 1000 times, and we calculated the decisive tools such as the average values of MLEs, biases, and MSEs (mean square error). The average values of MLEs, biases, and MSEs are obtained to illustrate the practical performance of the applied estimation method for the NLS-Weibull distribution. The decisive tools are calculated by using the R computer software with the "optim" function and the BFGS algorithm. The biases and MSEs with mathematical expression, respectively, are given by

$$Bias(\Theta) = \frac{1}{n}\sum_{i=1}^{n}\left(\hat{\Theta} - \Theta\right),$$

and

$$MSE(\Theta) = \frac{1}{n}\sum_{i=1}^{n}\left(\hat{\Theta} - \Theta\right)^2,$$

where, $\Theta = (\phi, \delta, \theta)$.

For numerical illustration, the simulation results of the average values of MLEs, Biases, and MSEs are recorded in Tables 1 and 2. Similarly, for more convenience to understand the simulation results, the average values of MLEs, biases, and MSEs are graphically illustrated in Figs. 6–9. Based on the facts given in Tables 1 and 2, and Figs. 6–9, we can see that as the sample size increases (i.e., $n \to \infty$), then

- The values of $\hat{\phi}_{MLE}$, $\hat{\delta}_{MLE}$, and $\hat{\theta}_{MLE}$ become closer to the true values.
- The MSE of $\hat{\phi}_{MLE}$, $\hat{\delta}_{MLE}$, and $\hat{\theta}_{MLE}$ decreases and approaches zero.
- The biases of $\hat{\phi}_{MLE}$, $\hat{\delta}_{MLE}$, and $\hat{\theta}_{MLE}$ declines to zero.

These results show that the corresponding MLE approach is consistent, asymptotically efficient, and also meets the invariance property.

Table 1: SS results of the NLS-Weibull distribution for Sets I and II

n	Est.	Set I: $\phi = 2.7, \delta = 3.7, \theta = 1.5$			Set II: $\phi = 1.7, \delta = 2.9, \theta = 0.6$		
		MLE	MSE	Bias	MLE	MSE	Bias
25	$\hat{\phi}$	2.893679	2.830421	0.193679	1.365718	2.232442	−0.334281
	$\hat{\delta}$	4.044985	0.889671	0.344985	2.967707	0.699697	0.067707
	$\hat{\theta}$	1.712273	0.406412	0.212273	0.747975	0.067491	0.147974
50	$\hat{\phi}$	2.968509	2.608663	0.268508	1.389979	1.747829	−0.310020
	$\hat{\delta}$	3.964951	0.742243	0.264950	2.841260	0.458464	−0.058739
	$\hat{\theta}$	1.631182	0.235434	0.131181	0.705689	0.042682	0.105688
75	$\hat{\phi}$	2.844804	2.424761	0.144804	1.355464	1.572647	−0.344536
	$\hat{\delta}$	3.884524	0.675238	0.184523	2.800423	0.392365	−0.099577
	$\hat{\theta}$	1.635384	0.200696	0.135384	0.699246	0.035425	0.099246
100	$\hat{\phi}$	2.950103	2.266705	0.250103	1.385043	1.362354	−0.314957
	$\hat{\delta}$	3.919226	0.647032	0.219226	2.802180	0.334703	−0.097819
	$\hat{\theta}$	1.592681	0.158746	0.092681	0.690605	0.031106	0.090605
200	$\hat{\phi}$	2.905332	2.007074	0.205332	1.357552	0.777895	−0.342447
	$\hat{\delta}$	3.855996	0.539114	0.155995	2.744179	0.200421	−0.155820
	$\hat{\theta}$	1.580694	0.131394	0.080694	0.667935	0.018197	0.067935
300	$\hat{\phi}$	2.808515	1.582507	0.108514	1.503251	0.434313	−0.196749
	$\hat{\delta}$	3.795668	0.406745	0.095668	2.811024	0.105556	−0.088975
	$\hat{\theta}$	1.570550	0.104628	0.070549	0.639525	0.010641	0.039525
400	$\hat{\phi}$	2.787404	1.358292	0.087403	1.533457	0.338887	−0.166543
	$\hat{\delta}$	3.775640	0.351479	0.075640	2.824072	0.082729	−0.075927
	$\hat{\theta}$	1.565028	0.089658	0.065028	0.631575	0.008061	0.031575
500	$\hat{\phi}$	2.760749	1.299881	0.060748	1.579260	0.193477	−0.120739
	$\hat{\delta}$	3.767451	0.338408	0.067450	2.844321	0.046573	−0.055679
	$\hat{\theta}$	1.567630	0.083511	0.067630	0.621785	0.005132	0.021785

(Continued)

Table 1 (continued)

n	Est.	Set I: $\phi = 2.7, \delta = 3.7, \theta = 1.5$			Set II: $\phi = 1.7, \delta = 2.9, \theta = 0.6$		
		MLE	MSE	Bias	MLE	MSE	Bias
600	$\hat{\phi}$	2.711095	1.189433	0.011094	1.588381	0.181613	−0.111618
	$\hat{\delta}$	3.733054	0.303505	0.033053	2.848550	0.044177	−0.051450
	$\hat{\theta}$	1.571135	0.080826	0.071134	0.619985	0.004612	0.019985
700	$\hat{\phi}$	2.718024	1.060423	−0.009696	1.651225	0.062308	−0.048775
	$\hat{\delta}$	3.738159	0.264616	0.016706	2.876572	0.015201	−0.023428
	$\hat{\theta}$	1.563374	0.069158	0.064438	0.608139	0.001681	0.008139
800	$\hat{\phi}$	2.731883	0.978679	0.045882	1.660465	0.057242	−0.039535
	$\hat{\delta}$	3.737696	0.251778	0.015696	2.881715	0.012960	−0.018285
	$\hat{\theta}$	1.551826	0.060030	0.051825	0.606955	0.001461	0.006955
900	$\hat{\phi}$	2.743707	0.891878	0.043706	1.668087	0.044872	−0.031912
	$\hat{\delta}$	3.739321	0.223604	0.012321	2.884707	0.011045	−0.015293
	$\hat{\theta}$	1.543186	0.054331	0.043185	0.605459	0.001277	0.005459
1000	$\hat{\phi}$	2.716166	0.890955	0.016166	1.683783	0.028260	−0.016216
	$\hat{\delta}$	3.724338	0.220139	0.010338	2.892949	0.006087	−0.007051
	$\hat{\theta}$	1.550280	0.059176	0.040280	0.603031	0.000699	0.003031

Table 2: SS results of the NLS-Weibull distribution for Sets III and IV

n	Est.	Set III: $\phi = 1.5$, $\delta = 3.7$, $\theta = 1.0$			Set IV: $\phi = 4.9$, $\delta = 0.6$, $\theta = 2.4$		
		MLEs	MSEs	Biases	MLEs	MSEs	Biases
25	$\hat{\phi}$	1.191130	1.508299	−0.571819	4.096000	2.881750	−0.803999
	$\hat{\delta}$	3.762875	0.733811	0.090129	0.470861	0.071131	−0.129139
	$\hat{\theta}$	1.168020	0.176571	0.256181	2.841220	0.771330	0.441219
50	$\hat{\phi}$	1.234604	1.442343	−0.308869	4.044432	2.736441	−0.855568
	$\hat{\delta}$	3.733957	0.523246	0.062875	0.477014	0.062803	−0.122986
	$\hat{\theta}$	1.137542	0.117013	0.168020	2.776756	0.612049	0.376756
75	$\hat{\phi}$	1.306533	1.237132	−0.265395	4.093423	2.510314	−0.806576
	$\hat{\delta}$	3.714568	0.417390	0.033956	0.482457	0.054066	−0.117543
	$\hat{\theta}$	1.112982	0.091529	0.137542	2.739282	0.523242	0.339281
100	$\hat{\phi}$	1.322303	1.281102	−0.193467	4.233777	1.902733	−0.666223
	$\hat{\delta}$	3.691194	0.384316	0.014568	0.504205	0.042283	−0.095794
	$\hat{\theta}$	1.098502	0.081121	0.112982	2.655649	0.362937	0.255649

(Continued)

Table 2 (continued)

n	Est.	Set III: $\phi = 1.5$, $\delta = 3.7$, $\theta = 1.0$			Set IV: $\phi = 4.9$, $\delta = 0.6$, $\theta = 2.4$		
		MLEs	MSEs	Biases	MLEs	MSEs	Biases
200	$\hat{\phi}$	1.331823	1.014800	−0.168177	4.306000	1.577376	−0.594000
	$\hat{\delta}$	3.677084	0.276519	−0.022916	0.516260	0.032202	−0.083739
	$\hat{\theta}$	1.089302	0.055209	0.089301	2.599332	0.254775	0.199331
300	$\hat{\phi}$	1.390722	0.957931	−0.109277	4.350624	1.443807	−0.549376
	$\hat{\delta}$	3.692957	0.243371	−0.007043	0.518368	0.028929	−0.081631
	$\hat{\theta}$	1.067582	0.046774	0.067582	2.594238	0.249702	0.194238
400	$\hat{\phi}$	1.372897	0.791042	−0.127102	4.437482	1.078511	−0.462518
	$\hat{\delta}$	3.668421	0.199318	−0.031579	0.533651	0.022171	−0.066349
	$\hat{\theta}$	1.065321	0.039446	0.065321	2.545006	0.163616	0.145006
500	$\hat{\phi}$	1.388746	0.718021	−0.111254	4.479133	0.868135	−0.420867
	$\hat{\delta}$	3.672308	0.172682	−0.027692	0.541776	0.017707	−0.058224
	$\hat{\theta}$	1.058569	0.034340	0.058568	2.513402	0.112680	0.113402
600	$\hat{\phi}$	1.365965	0.599025	−0.134034	4.548946	0.665782	−0.351054
	$\hat{\delta}$	3.657663	0.150207	−0.042337	0.549079	0.014031	−0.050920
	$\hat{\theta}$	1.056063	0.029487	0.056063	2.497175	0.092027	0.097174
700	$\hat{\phi}$	1.398934	0.526163	−0.101065	4.599100	0.486968	−0.300899
	$\hat{\delta}$	3.680304	0.123178	−0.019696	0.558541	0.010401	−0.041459
	$\hat{\theta}$	1.048054	0.025834	0.048054	2.468251	0.051178	0.068250
800	$\hat{\phi}$	1.444761	0.546114	−0.055239	4.592541	0.546330	−0.307459
	$\hat{\delta}$	3.692570	0.125991	−0.007430	0.556212	0.011195	−0.043788
	$\hat{\theta}$	1.037813	0.023614	0.037813	2.477539	0.065010	0.077539
900	$\hat{\phi}$	1.415912	0.457824	−0.084088	4.616026	0.412653	−0.283973
	$\hat{\delta}$	3.675788	0.101939	−0.024211	0.559129	0.008800	−0.040870
	$\hat{\theta}$	1.039296	0.021217	0.039296	2.465173	0.045908	0.065173
1000	$\hat{\phi}$	1.4258967	0.400934	−0.074103	4.645025	0.377972	−0.254975
	$\hat{\delta}$	3.677558	0.088628	−0.022442	0.561374	0.008164	−0.038625
	$\hat{\theta}$	1.035343	0.018514	0.035343	2.462610	0.036805	0.062610

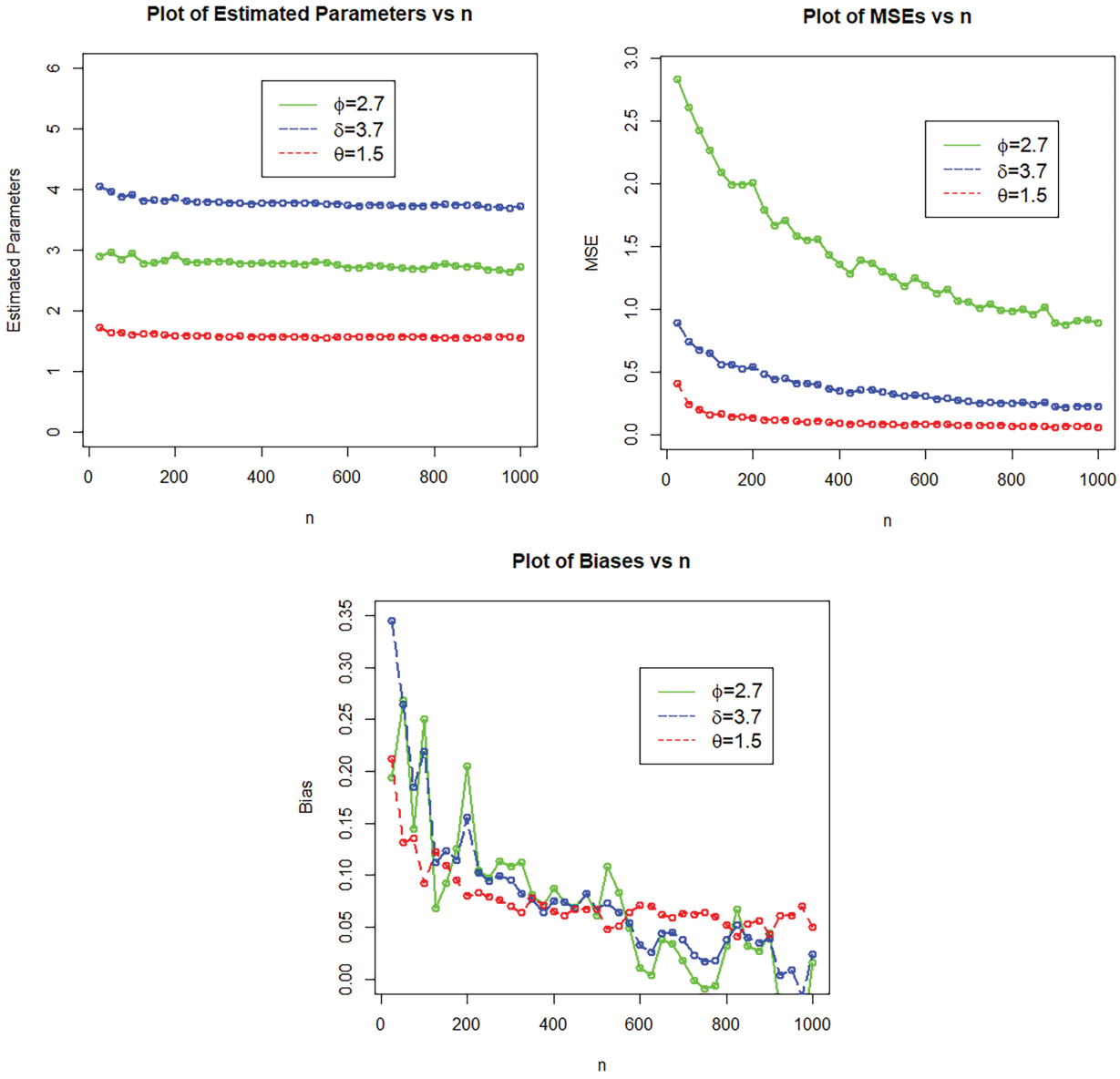

Figure 6: The simulation results (visual representation) of the NLS-Weibull distribution for Set I

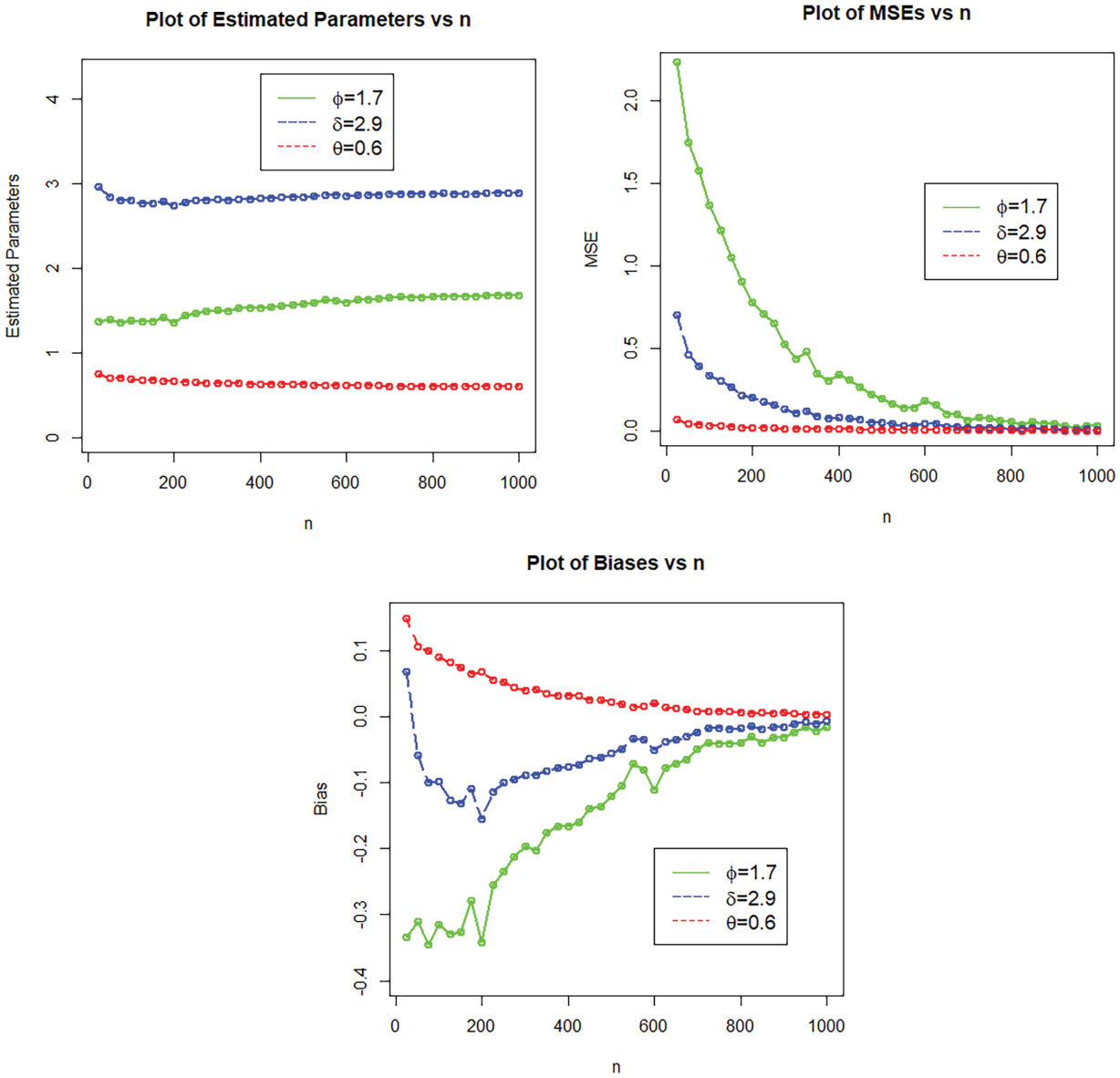

Figure 7: The simulation results (visual representation) of the NLS-Weibull distribution for Set II

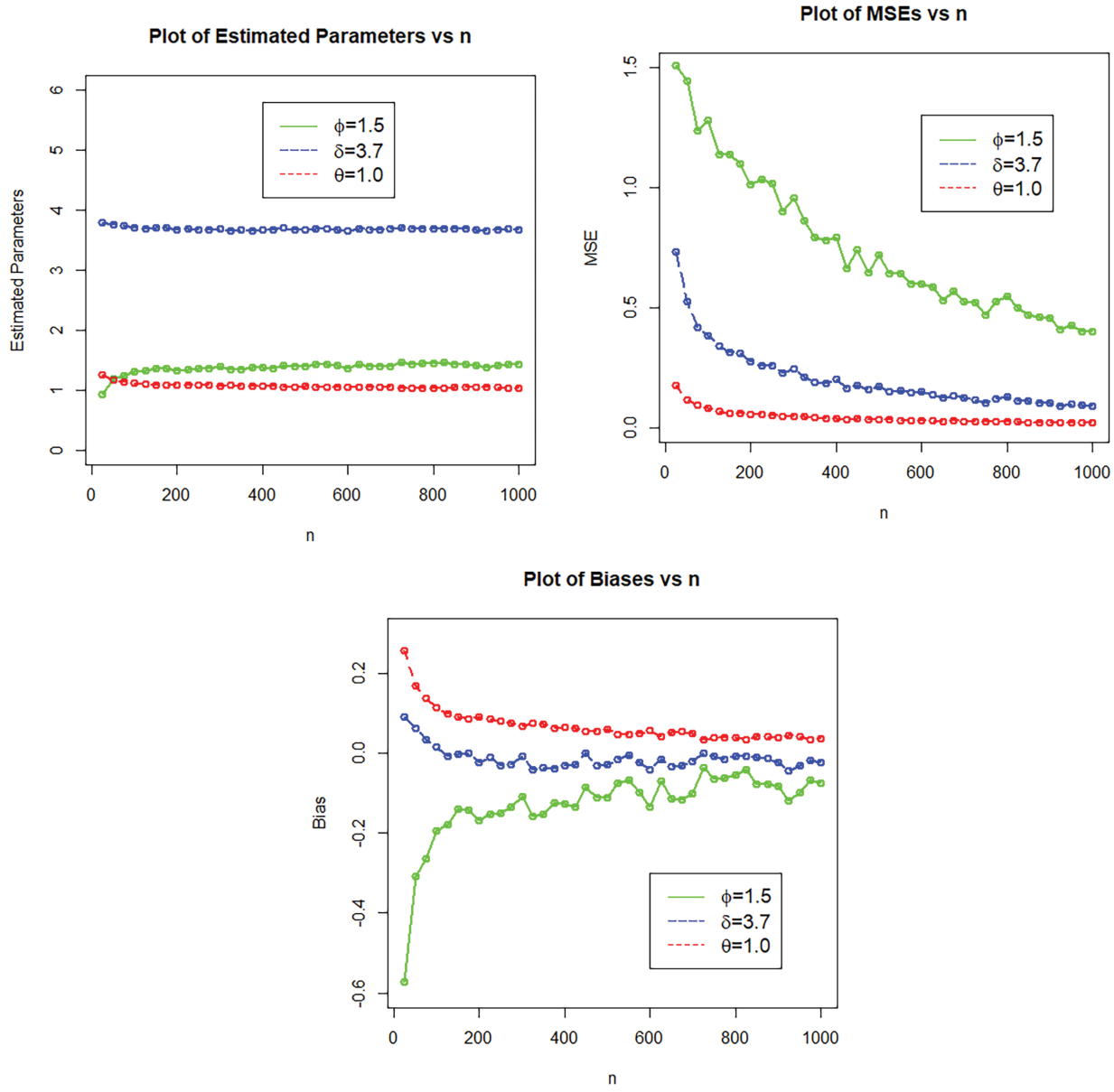

Figure 8: The simulation results (visual representation) of the NLS-Weibull distribution for Set III

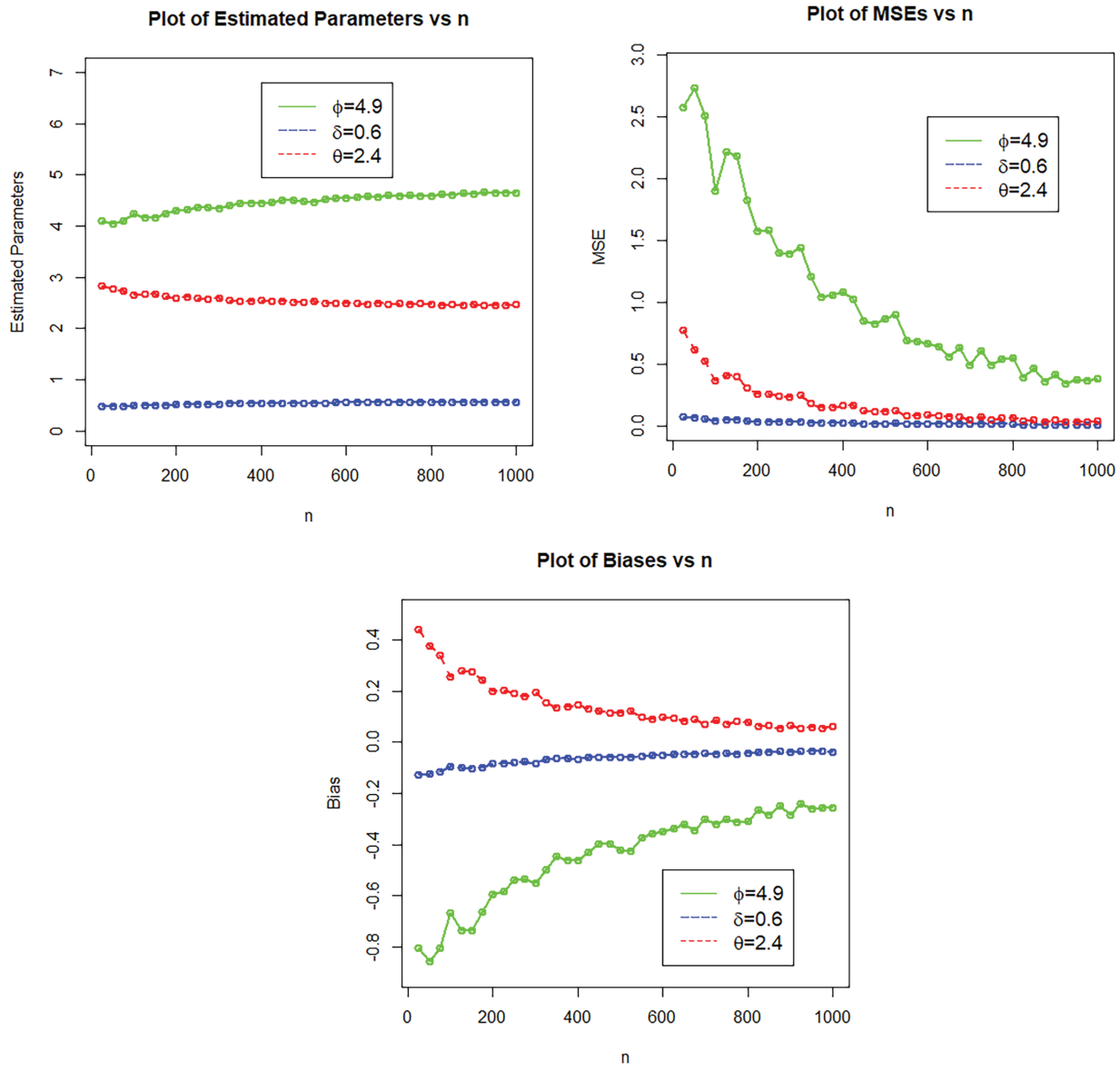

Figure 9: The simulation results (visual representation) of the NLS-Weibull distribution for Set IV

6 Application of the NLS-Weibull Distribution

In this section of the article, we observe the practical performance of the NLS-Weibull distribution based on four real data sets from the field of reliability engineering. The first data set (onward indicated by DASE 1) represents the failure time of electronic devices and is presented in Table 3 with reference. The second data set (onward indicated by DASE 2) is civil engineering data, representing the breaking stress of carbon fibers, and presented in Table 3 with reference. The third data set (onward indicated by DASE 3) represents the strengths of 1.5 cm glass fibers, which were originally obtained by workers at the UK (National Physical Laboratory) and presented in Table 3 with references. The fourth data

set (onward indicated by DASE 4) represents single-carbon fibers and impregnated 1000-carbon fiber tows and is recorded in Table 3 with references.

Table 3: Engineering data sets

No.	Observations	Source
DASE 1	7.89, 4.69, 4.20, 3.34, 3.03, 3.03, 2.33, 2.17, 2.14, 2.05, 2.02, 1.81, 1.80, 1.80, 1.64, 1.63, 1.60, 1.58, 1.55, 1.54, 1.54, 1.53, 1.52, 1.51, 1.50, 1.45, 1.43, 1.40, 1.34, 1.33, 1.31, 1.29, 1.20, 1.18, 1.15, 1.11, 1.10, 1.10, 1.05, 1.03, 1.02, 1.01, 1.00, 0.99, 0.95, 0.92, 0.90, 0.85, 0.83, 0.80, 0.80, 0.79, 0.79, 0.73, 0.72, 0.72, 0.72, 0.68, 0.67, 0.65, 0.63, 0.60, 0.60, 0.56, 0.54, 0.52, 0.43, 0.42, 0.40, 0.38, 0.36, 0.35, 0.34, 0.29, 0.24, 0.24, 0.23, 0.20, 0.19, 0.18, 0.13, 0.12, 0.11, 0.11, 0.10, 0.10, 0.09, 0.09, 0.08, 0.07, 0.07, 0.06, 0.05, 0.04, 0.03, 0.03, 0.02, 0.02, 0.02, 0.01, 0.01.	Chamunorwaet et al. (2021) [28]
DASE 2	5.56, 5.08, 4.91, 4.90, 4.70, 4.42, 4.38, 4.20, 3.75, 3.70, 3.68, 3.68, 3.68, 3.65, 3.60, 3.56, 3.51, 3.39, 3.39, 3.33, 3.31, 3.31, 3.28, 3.27, 3.22, 3.22, 3.19, 3.19, 3.15, 3.15, 3.11, 3.11, 3.09, 2.97, 2.97, 2.96, 2.95, 2.93, 2.88, 2.87, 2.85, 2.83, 2.82, 2.81, 2.81, 2.79, 2.77, 2.76, 2.74,2.73, 2.67, 2.59, 2.56, 2.55, 2.55, 2.53, 2.50, 2.48, 2.48, 2.43, 2.41, 2.38, 2.35, 2.17, 2.17, 2.17, 2.12, 2.05, 2.03, 2.03, 2.00, 1.92, 1.89, 1.87, 1.84, 1.84, 1.80, 1.73, 1.71, 1.69, 1.69, 1.61, 1.61, 1.59, 1.59, 1.57, 1.57, 1.47, 1.41, 1.36, 1.25, 1.22, 1.18, 1.17, 1.12, 1.08, 0.98, 0.85, 0.81, 0.39.	Alnssyan et al. (2023) [29]
DASE 3	0.55, 0.74, 0.77, 0.81, 0.84,0.93, 1.04, 1.11, 1.13, 1.24, 1.25, 1.27, 1.28, 1.29, 1.30, 1.36, 1.39, 1.42, 1.48, 1.48, 1.49,1.49, 1.50, 1.50, 1.51, 1.52, 1.53, 1.54, 1.55, 1.55, 1.58, 1.59, 1.60, 1.61, 1.61, 1.61, 1.61, 1.62, 1.62, 1.63, 1.64, 1.66, 1.66, 1.66, 1.67, 1.68, 1.68, 1.69, 1.70, 1.70, 1.73, 1.76, 1.76,1.77, 1.78, 1.81, 1.82, 1.84, 1.84, 1.89, 2.00, 2.01, 2.24.	Dey et al. (2017) [13]
DASE 4	0.0312, 0.314, 0.479, 0.552, 0.700, 0.803, 0.861, 0.865, 0.944, 0.958, 0.966, 0.977, 1.006, 1.021, 1.027, 1.055, 1.063, 1.098, 1.140, 1.179, 1.224, 1.240, 1.253, 1.270, 1.272, 1.274, 1.301, 1.301, 1.359, 1.382, 1.382, 1.426, 1.434, 1.435, 1.478, 1.490, 1.511, 1.514, 1.535, 1.554, 1.566, 1.570, 1.586, 1.629, 1.633, 1.642, 1.648, 1.684, 1.697, 1.726, 1.770, 1.773, 1.800, 1.809, 1.818, 1.821, 1.848, 1.880, 1.954, 2.012, 2.067, 2.084, 2.090, 2.096, 2.128, 2.233, 2.433, 2.585, 2.585.	Nagarjuna et al. (2021) [30]

Using each considered data set and the flexibility and superiority of the NLS-Weibull are compared with four well-known distributions, including Kumaraswamy Weibull (K-Weibull) distribution of Cordeiro et al. (2010) [31], Weibull distribution proposed of Weibull (1951) [32], exponentiated Weibull (E-Weibull) distribution of Mudholkar and Srivastava (1993) [2], New generalized Logarithmic Weibull (NGL-Weibull) distributions of Shah et al. (2023) [25], New Exponent Weibull (NE-Weibull) of Shah et al. (2022) [33], and Flexible Reduced Logarithmic Weibull (FRL-Weibull) distribution of Liu et al. (2020) [34]. The SFs of K-Weibull, Weibull, E-Weibull, NGL-Weibull, NE-Weibull, and FRL-Weibull distributions are given by

- The K-Weibull distribution

$$S(t;a,b,\delta,\theta) = \left[1-\left(1-e^{-\delta t^{\theta}}\right)^{a}\right]^{b} a,b,\delta,\theta \in \Re^{+} \quad t \in \Re^{+}.$$

- The Weibull distribution

$$S(t;\delta,\theta) = e^{-\delta t^{\theta}} \delta,\theta \in \Re^{+} \quad t \in \Re^{+}.$$

- The E-Weibull distribution

$$S(t;\delta,\theta) = 1-\left(1-e^{-\delta t^{\theta}}\right)^{\phi} \delta,\theta \in \Re^{+} \quad t \in \Re^{+}.$$

- The NGL-Weibull distribution

$$S(t;\phi,\delta,\theta) = 1-\frac{e^{\phi}\left(1-e^{-\delta t^{\theta}}\right)}{\left[e-\log\left(1-e^{-\delta t^{\theta}}\right)\right]^{\phi}} \phi,\delta,\theta \in \Re^{+} \quad t \in \Re^{+}.$$

- The NE-Weibull distribution

$$S(t;\delta,\theta) = \left(\frac{e^{e^{-\delta t^{\theta}}}-1}{e-e^{e^{-\delta t^{\theta}}}}\right) \phi,\delta,\theta \in \Re^{+} \quad t \in \Re^{+}.$$

- The FRL-Weibull distribution

$$S(t;\phi,\delta,\theta) = \frac{\log\left[\phi+1-\phi\left(1-e^{-\delta t^{\theta}}\right)\right]}{\log(1+\phi)} \phi,\delta,\theta \in \Re^{+} \quad t \in \Re^{+}.$$

After choosing the different well-known competing distributions, we proceed with discrimination and goodness of fit measures along with their corresponding p-values. The discrimination measures consist of Akaike information (AI, hereafter designated by DM_1), Bayesian information (BI, onward designated by DM_2), consistent Akaike information (CAI, hereafter designated by DM_3), and Hannan Quinn information (HQI, onward designated by DM_4). Similarly, the goodness of fit measures consist of Cramer von Mises (CVM, hereafter designated by GM_1), Anderson Darling (AD, hereafter designated by GM_2), Kolmogorov-Smirnov (KS, hereafter designated by GM_3), and their corresponding p-values. The above analytical measures formulas, respectively, are given by

- The AI evaluation criteria
  $DM_1 = 2x - 2\ell(\omega)$;

- The BI evaluation criteria
  $DM_2 = x\log(w) - 2\ell(\omega)$;

- The CAI evaluation criteria
  $DM_3 = \dfrac{2wx}{w-x-1} - 2\ell(\omega)$;

- The HQI evaluation criteria
  $DM_4 = 2x\log[\log(w)] - 2\ell(\omega)$;

- The CVM evaluation criteria
  $GM_1 = \sum_{i=1}^{w}\left(F(t_i) - \dfrac{2i-1}{2w}\right)^2 + \dfrac{1}{12w}$;

- The AD evaluation criteria
  $GM_2 = -w - \dfrac{1}{w}\sum_{i=1}^{w}(2i-1)\times\left\{\log\left[1-F\left(t_{(i-w+1)}\right)\right] + \log\left[F\left(t_{(i)}\right)\right]\right\}$;

- The KS evaluation criteria
  $GM_3 = \underset{i=1,2,3\ldots w}{Max}\left[\left(\dfrac{i}{w} - F\left(t_{(i)}\right)\right), \left(F\left(t_{(i)}\right) - \dfrac{i-1}{w}\right)\right]$.

The above analytical measures process is carried out using the R computer software with the AdequacyModel package and the BFGS algorithm. Using four engineering data sets, we compare the NLS-Weibull distribution with other competing distributions. Generally speaking, in the comparison process, a model with the smallest values of the above analytical measures and the largest p-value will be considered a good competitor for the respective dataset. Based on these evaluation criteria, it is concluded that the NLS-Weibull distribution has the lowest values of DM_1, DM_2, DM_3, DM_4, GM_1, GM_2, and GM_3, and the highest p-value.

6.1 Illustrative Example Using Engineering DASE 1

Some basic descriptive measures of DASE 1 are: min. = 0.010, 1st Qu. = 0.240, median = 0.800, mean = 1.025, 3rd Qu. = 1.450, max. = 7.890, skewness = 3.001719, kurtosis = 16.70899, variance = 1.252985, and range = 7.88. Furthermore, using DASE 1, the Box plot, Violin plot, and TTT-plot are sketched in Fig. 10.

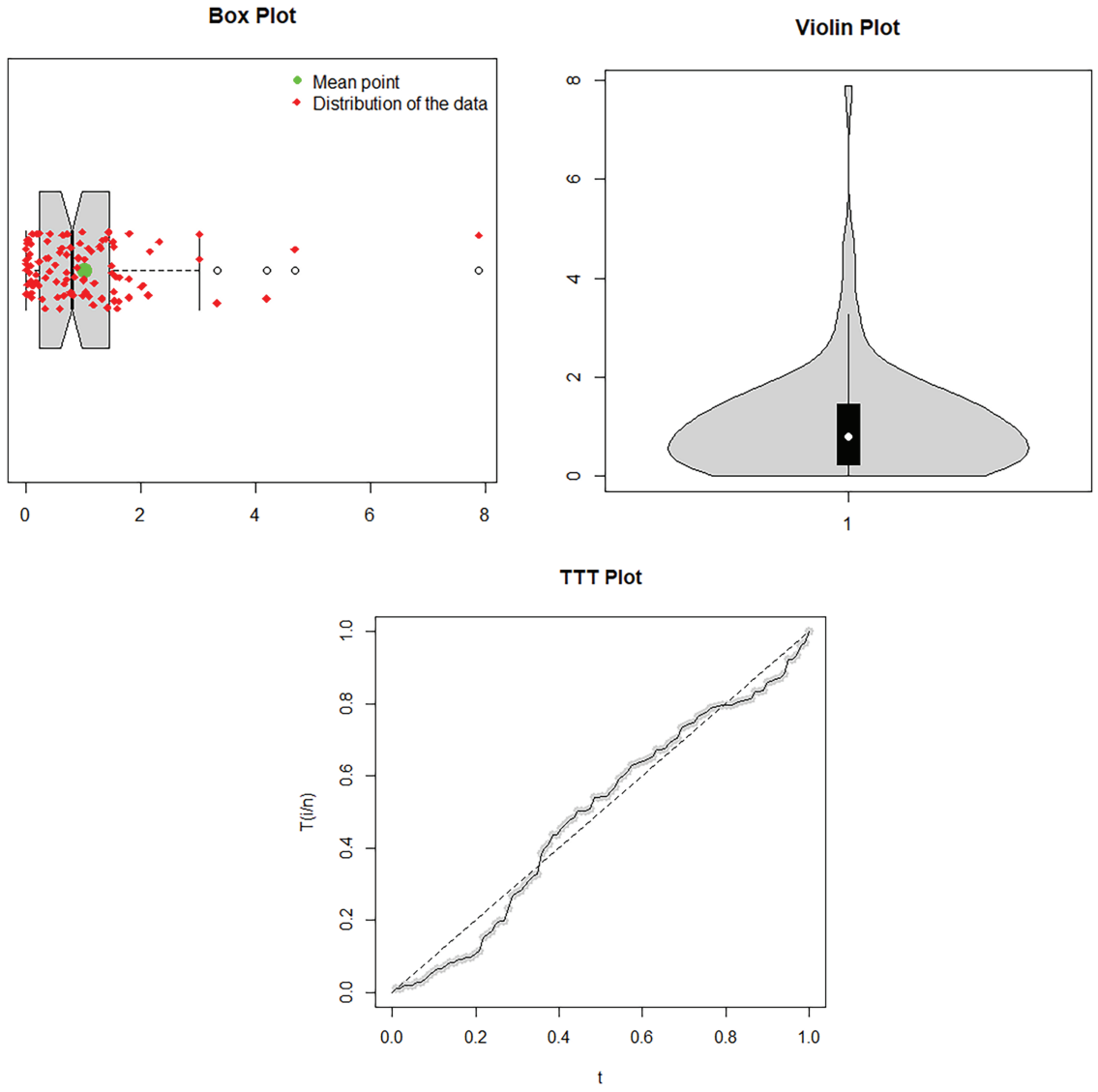

Figure 10: The Box plot, Violin plot, and TTT plot of the DASE 1

Corresponding to DASE 1, the MLEs values (i.e., $\hat{\phi}_{MLE}$, $\hat{\delta}_{MLE}$, $\hat{\theta}_{MLE}$, $\hat{a}_{MLE}$, and $\hat{b}_{MLE}$) are recorded in Table 4. Furthermore, for visual illustration, the profile log-likelihood function plots of each estimated parameter value of the NLS-Weibull distribution are plotted in Fig. 11. These profile log-likelihood plots show that the estimated values of the parameter for the corresponding data set are the unique root and local maximum because they maximize the LLF (log likelihood function) of the NLS-Weibull distribution.

Table 4: The MLE values of the fitted distributions for the DASE 1

Distributions	$\hat{\phi}_{MLE}$	$\hat{\delta}_{MLE}$	$\hat{\theta}_{MLE}$	$\hat{a}_{MLE}$	$\hat{b}_{MLE}$
NLS-Weibull	0.9410235	0.9088493	0.7260288	–	–
Weibull	–	1.0093933	0.9258921	–	–
K-Weibull	–	0.3889217	0.1839456	0.08959719	0.40442875
E-Weibull	0.7929566	0.8113026	1.0604201	–	–
NGL-Weibull	0.1477606	0.9681163	0.9463988	–	–
FRL-Weibull	13.2918240	2.0245977	0.7436643	–	–
NE-Weibull	–	0.5687699	1.0421747	–	–

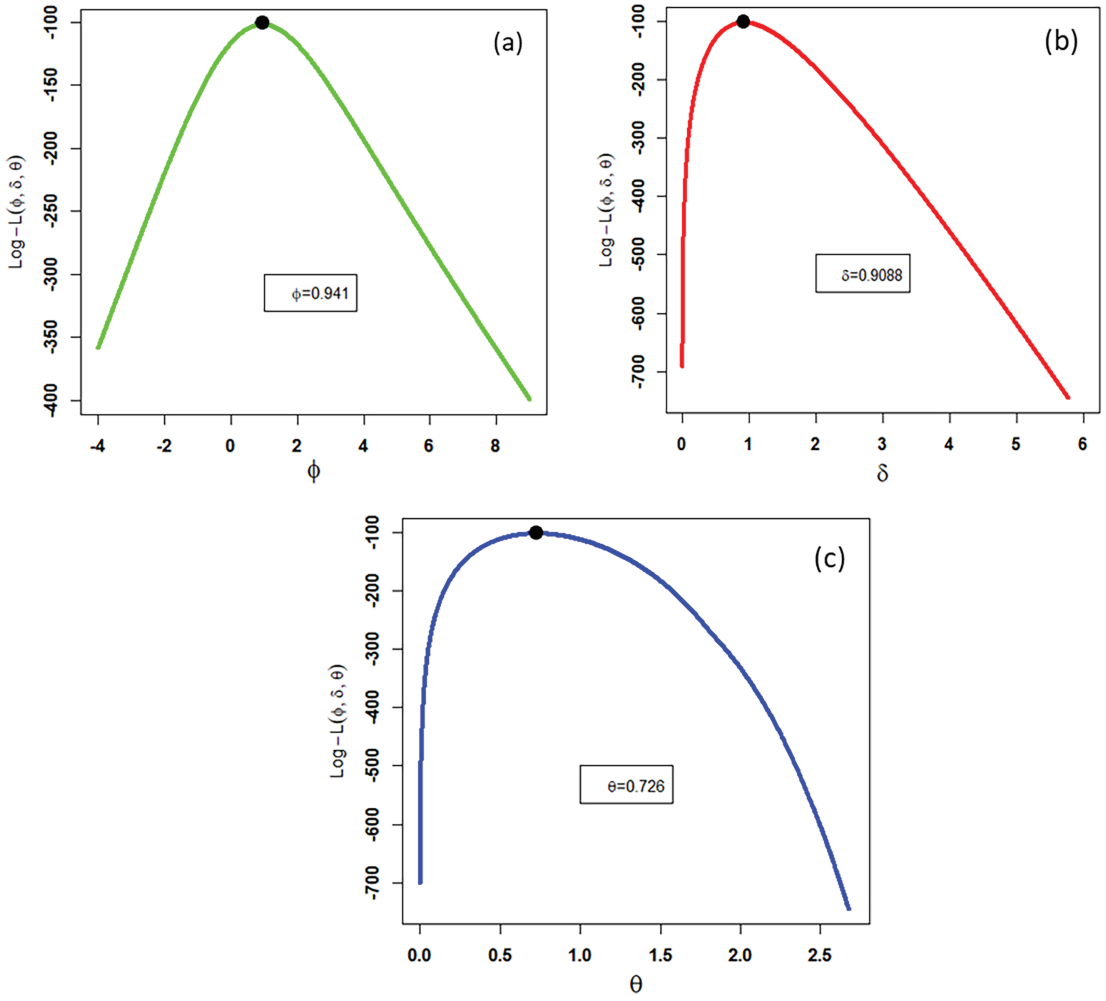

Figure 11: The profile log-likelihood plots of **(a)** $\hat{\phi}_{MLE}$, **(b)** $\hat{\delta}_{MLE}$, and **(c)** $\hat{\theta}_{MLE}$ of the NLS-Weibull distribution for DASE 1

Using DASE 1, the numerical values of the goodness of fit measures (i.e., GM_1, GM_2, and GM_3) and p-values of the fitted distributions are recorded in Table 5. Similarly, the numerical values of the discrimination measures (i.e., DM_1, DM_2, DM_3, and DM_4) are recorded in Table 6. Furthermore, to verify the flexibility and superiority of the NLS-Weibull distribution for the DASE 1, the fitted PDF plot, empirical CDF plot, fitted SF plot, and QQ plot are visually illustrated in Fig. 12. Hence, from Tables 5 and 6, we can clearly see that all the GM_1, GM_2, GM_3, DM_1, DM_2, and DM_3 values of the NLS-Weibull distribution are smaller than the competing distributions. Besides, if we look at the p-values of the fitted distributions, the p-value of the NLS-Weibull distribution is also higher than the other competing distributions. Similarly, based on the graphical illustrations (i.e., Figs. 11 and 12), we can also see that the newly proposed NLS-Weibull distribution has a close fit to the corresponding DASE 1.

Table 5: The goodness of fit criteria of the fitted distributions for DASE 1

Distributions	GM_1	GM_2	GM_3	p-values
NLS-Weibull	0.1314992	0.7944267	0.069681	0.7108
Weibull	0.1986618	1.1111238	0.090639	0.3778
K-Weibull	0.1454732	0.8694495	0.078016	0.5703
E-Weibull	0.1652423	0.9586438	0.084401	0.4680
NGL-Weibull	0.1974151	1.1053383	0.090756	0.3763
FRL-Weibul	0.1970089	0.8861431	0.072886	0.6567
NE-Weibull	0.2824784	1.5328579	0.10117	0.2525

Table 6: The discrimination measures of the fitted distributions for DASE 1

Distributions	DM_1	DM_2	DM_3	DM_4
NLS-Weibull	207.0456	214.8913	208.2931	210.2217
Weibull	209.9536	215.1839	210.0761	212.0719
K-Weibull	213.2601	223.7206	213.6767	217.4948
E-Weibull	211.5743	219.4197	211.8218	214.7504
NGL-Weibull	211.9445	219.7899	212.1927	215.1206
FRL-Weibull	209.5861	217.4315	209.8335	212.7621
NE-Weibull	213.0176	218.2472	213.1395	215.1344

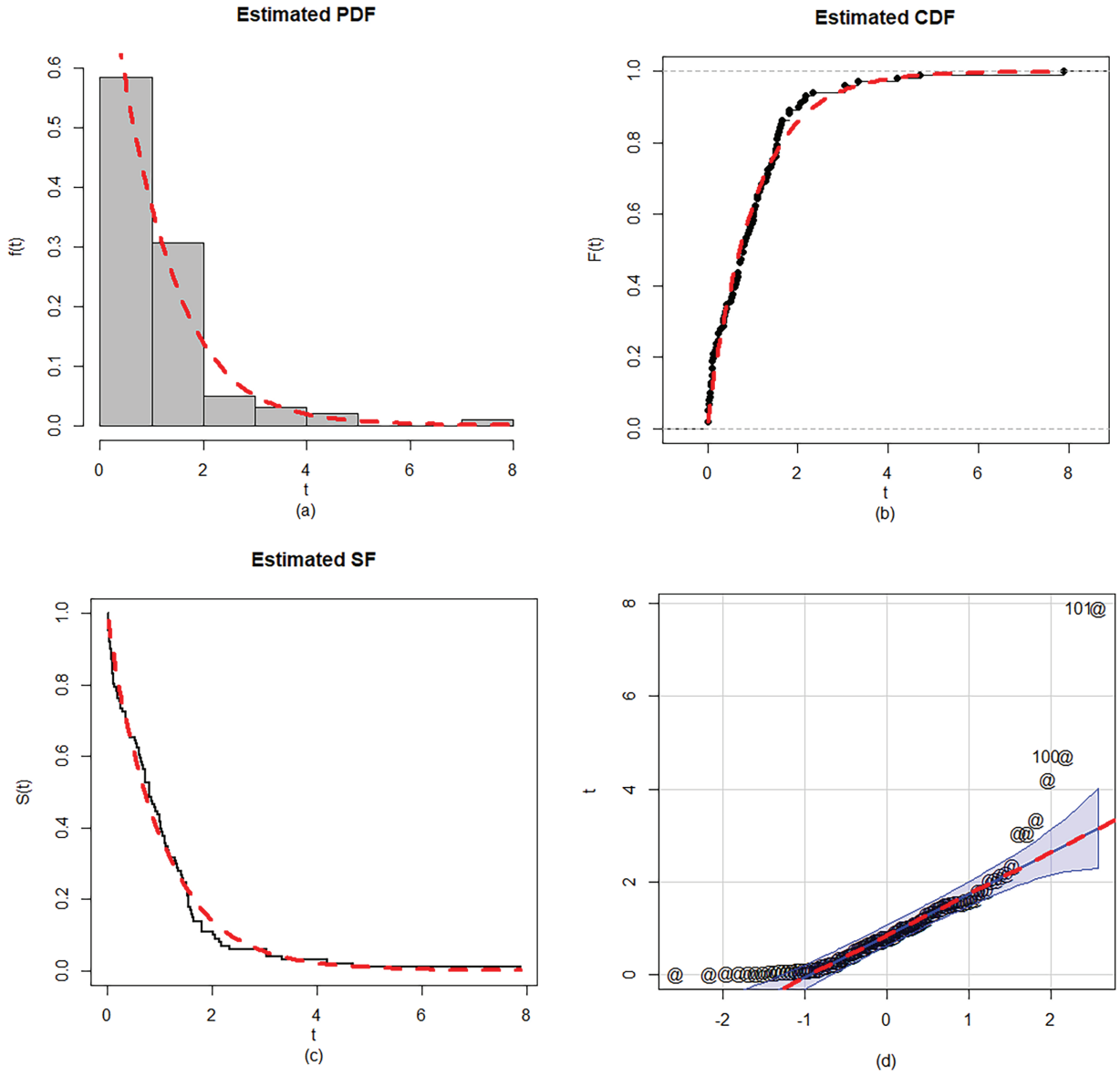

Figure 12: Visual illustration using DASE 1 (**a**) estimated PDF plot, (**b**) estimated CDF plot, (**c**) estimated SF plot, and (**d**) Q-Q plot of the NLS-Weibull distribution using DASE 1

6.2 Illustrative Example Using Civil Engineering DASE 2

Some basic descriptive measures of DASE 2 are: min. = 0.390, 1st Qu. = 1.840, median = 2.700, mean = 2.621, 3rd Qu. = 3.220, max. = 5.560, skewness = 0.3681541, kurtosis = 3.104939, variance = 1.027964, and range = 5.17. Furthermore, using DASE 2, the Box plot, Violin plot, and TTT-plot are sketched in Fig. 13.

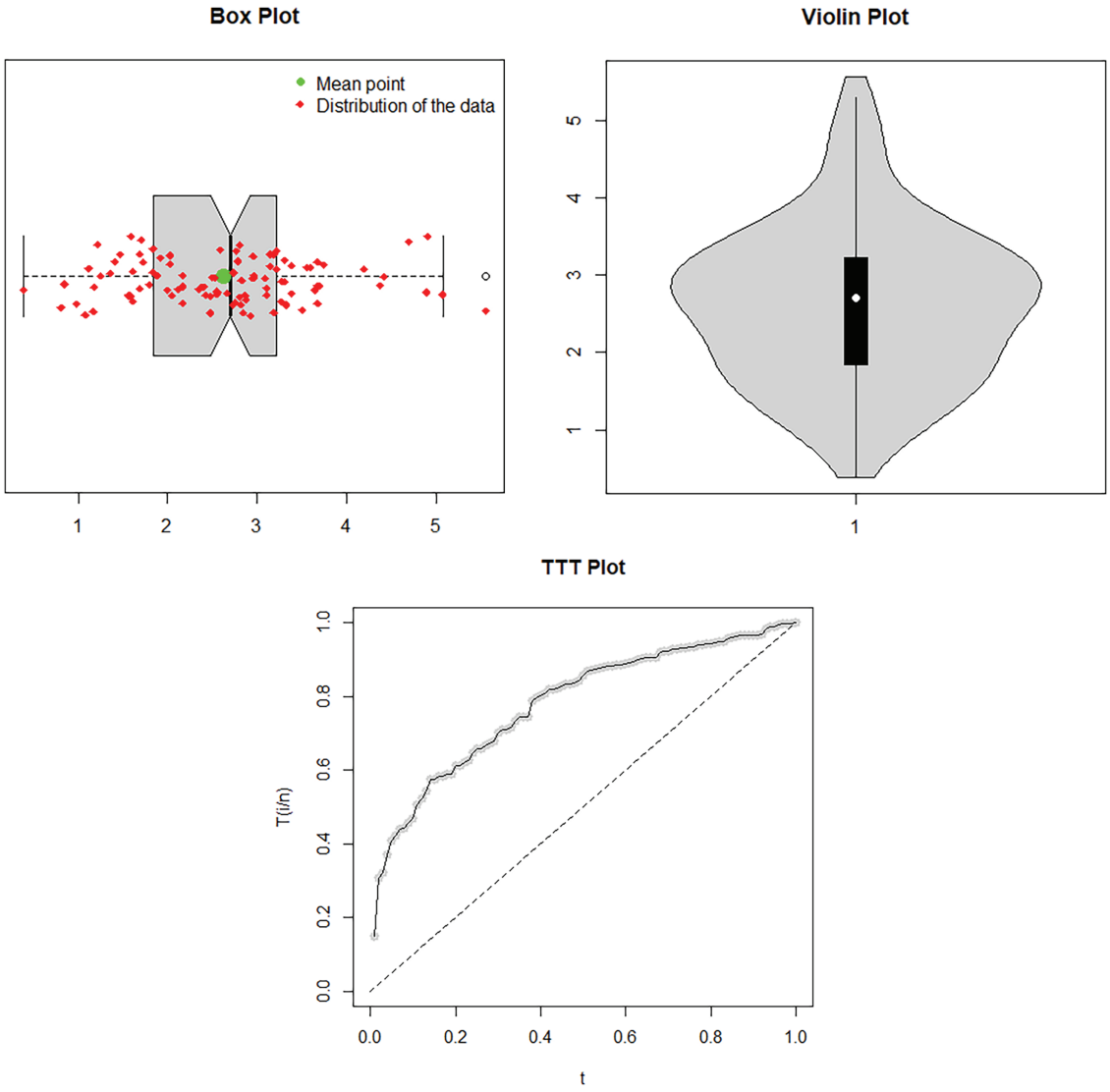

Figure 13: The Box, violin, and TTT plots for the DASE 2

Corresponding to DASE 2, the MLE values (i.e., $\hat{\phi}_{MLE}$, $\hat{\delta}_{MLE}$, $\hat{\theta}_{MLE}$, $\hat{a}_{MLE}$, and $\hat{b}_{MLE}$) are recorded in Table 7. Additionally, for visual illustration, the profile log-likelihood function plots of the estimated parameter value of the NLS-Weibull distribution are plotted in Fig. 14. These profile log-likelihood plots confirmed that the estimated values of the parameter for the DASE 2 are the unique root and local maximum because they maximize the LLF of the NLS-Weibull distribution.

Table 7: The MLE values of the fitted distributions for the DASE 2

Distributions	$\hat{\phi}_{MLE}$	$\hat{\delta}_{MLE}$	$\hat{\theta}_{MLE}$	$\hat{a}_{MLE}$	$\hat{b}_{MLE}$
NLS-Weibull	4.0022009	0.5333664	1.3041125	–	–
Weibull	–	0.0490731	2.7920671	–	–
K-Weibull	–	0.0779501	2.3291778	1.3954721	1.3588384
E-Weibull	1.3197872	0.0932791	2.4060962	–	–
NGL-Weibull	2.0335104	0.1387762	2.1932717	–	–
FRL-Weibull	0.29285149	0.03941507	2.89748705	–	–
NE-Weibull	–	0.01798243	3.20185047	–	–

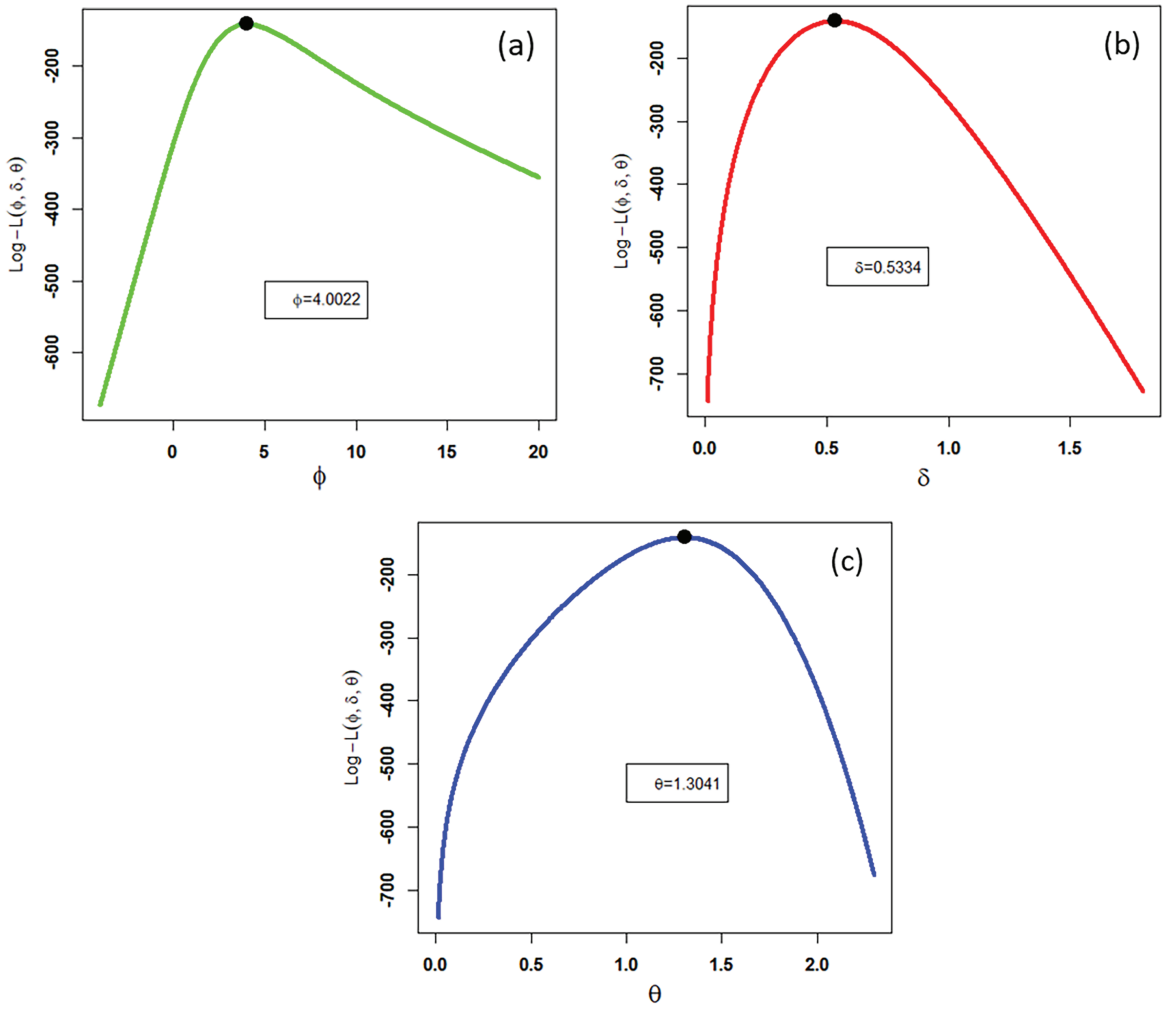

Figure 14: The profile log-likelihood plots of (**a**) $\hat{\phi}_{MLE}$, (**b**) $\hat{\delta}_{MLE}$, and (**c**) $\hat{\theta}_{MLE}$ of the NLS-Weibull distribution for DASE 2

Using DASE 2, the numerical values of the goodness of fit measures (i.e., GM_1, GM_2, and GM_3) and p-values of the fitted distributions are recorded in Table 8. Similarly, the numerical values of the discrimination measures (i.e., DM_1, DM_2, DM_3, and DM_4) are recorded in Table 9. Furthermore, to verify the flexibility and superiority of the NLS-Weibull distribution for the DASE 2, the fitted PDF plot, empirical CDF plot, fitted SF plot, and QQ plot are visually illustrated in Fig. 15. Hence, from Tables 8 and 9, we can clearly see that all the GM_1, GM_2, GM_3, DM_1, DM_2, and DM_3 values of the NLS-Weibull distribution are smaller than those of the competing distributions. Besides, if we look at the p-values of the fitted distributions, the p-value of the NLS-Weibull distribution is also higher than the competing distributions. Similarly, based on the graphical illustrations (i.e., Figs. 14 and 15), we can also see that the NLS-Weibull distribution has a close fit to the corresponding DASE 2.

Table 8: The goodness-of-fit criteria of the fitted distributions for DASE 2

Distributions	GM_1	GM_2	GM_3	p-values
NLS-Weibull	0.05355433	0.3940793	0.055132	0.9215
Weibull	0.06227696	0.4157641	0.060521	0.8573
K-Weibull	0.07032307	0.4119221	0.064434	0.8007
E-Weibull	0.07046344	0.4133445	0.064528	0.7994
NGL-Weibull	0.06865903	0.4008817	0.064549	0.7990
FRL-Weibull	0.06579976	0.4216059	0.061367	0.8457
NE-Weibull	0.08182638	0.4482269	0.069941	0.7122

Table 9: The discrimination measures of the fitted distributions for DASE 2

Distributions	DM_1	DM_2	DM_3	DM_4
NLS-Weibull	285.3728	290.1884	285.6228	289.5359
Weibull	287.0586	292.2698	287.1823	290.1673
K-Weibull	290.8542	301.2748	291.2752	295.0716
E-Weibull	288.6641	296.4796	288.9141	291.8272
NGL-Weibull	288.5565	296.3720	288.8065	291.7195
FRL-Weibull	289.0135	296.8291	289.2635	292.1766
NE-Weibull	287.7262	291.9365	287.8499	290.8349

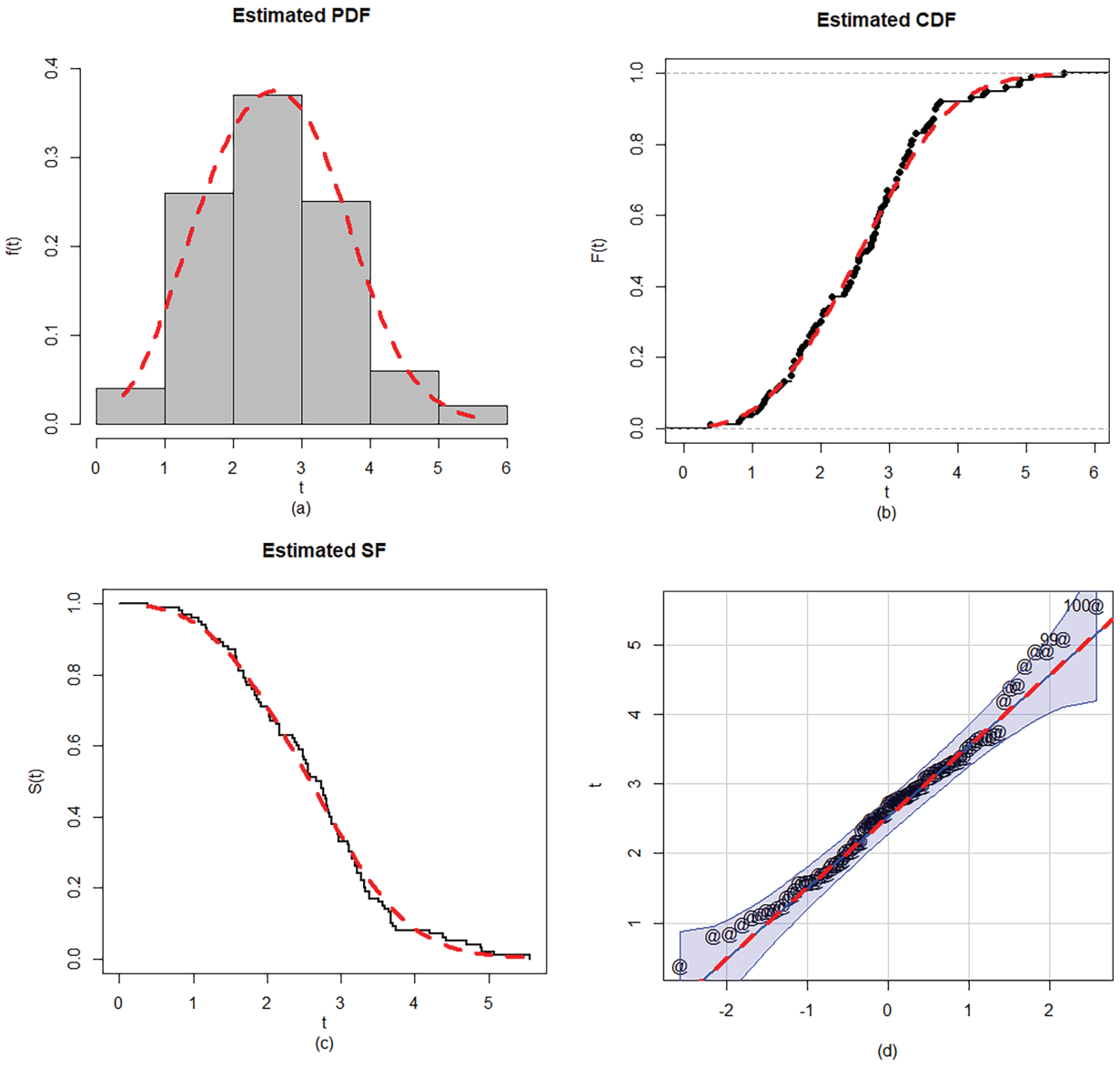

Figure 15: Visual illustration of the (**a**) estimated PDF plot, (**b**) estimated CDF plot, (**c**) estimated SF plot, and (**d**) Q-Q plot of the NLS-Weibull distribution using DASE 2

6.3 Illustrative Example Using Glass Fibers DASE 3

For the DASE 3, some basic descriptive measures are: min. = 0.550, 1st Qu. = 1.375, median = 1.590, mean = 1.507, 3rd Qu. = 1.685, max. = 2.240, skewness = −0.8999263, kurtosis = 3.923761, variance = 0.1050575, and range = 1.69. Furthermore, using DASE 3, the Box plot, Violin plot, and TTT-plot are sketched in Fig. 16.

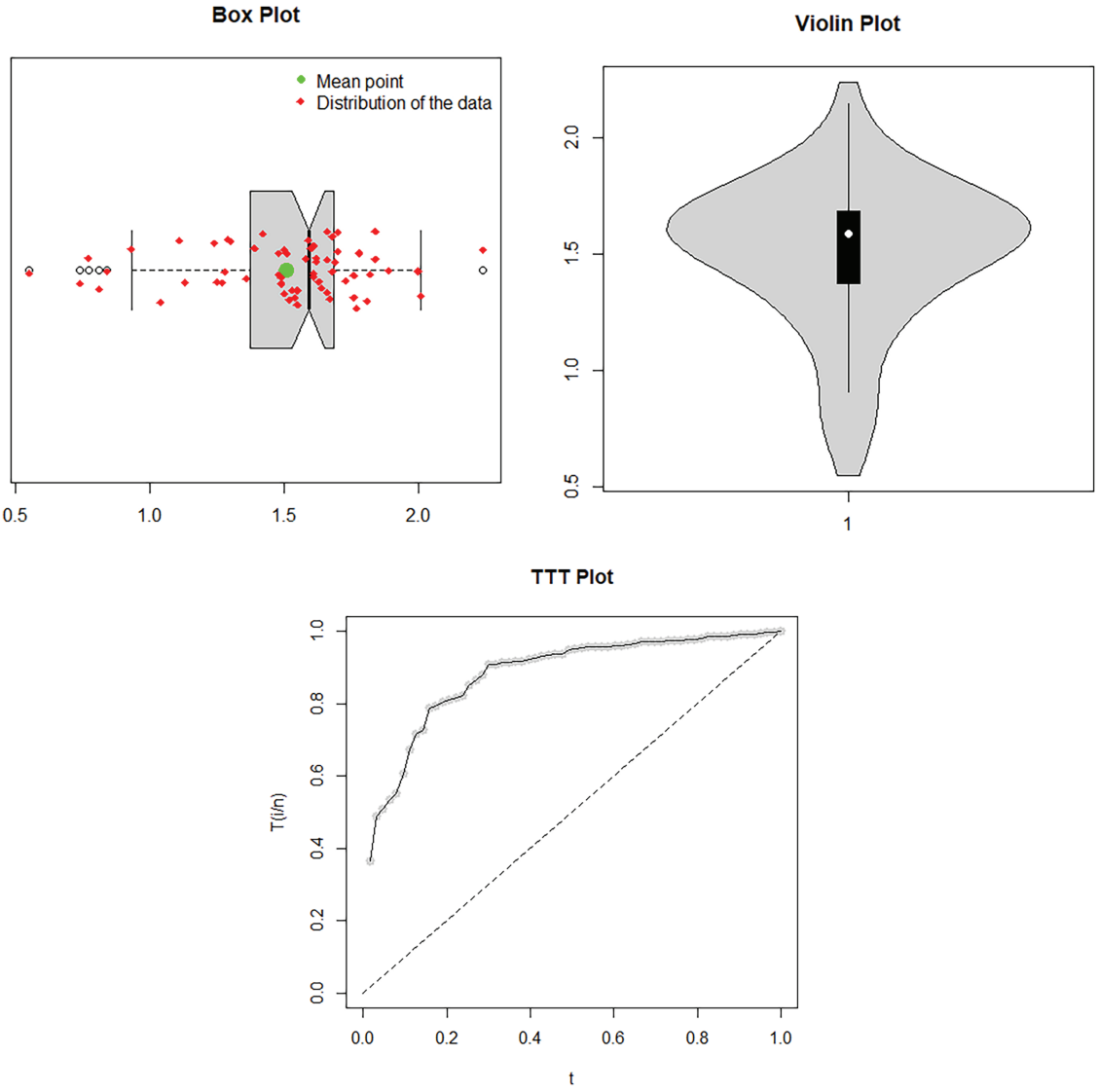

Figure 16: The Box, violin, and TTT plots for the DASE 3

Corresponding to DASE 3, the MLEs values (i.e., $\hat{\phi}_{MLE}$, $\hat{\delta}_{MLE}$, $\hat{\theta}_{MLE}$, $\hat{a}_{MLE}$, and $\hat{b}_{MLE}$) are recorded in Table 10. Additionally, for visual illustration, the profile log-likelihood function plots of each estimated parameter value of the NLS-Weibull distribution are plotted in Fig. 17. These profile log-likelihood plots demonstrated that the estimated values of the parameter for the corresponding data set are the unique root and local maximum because they maximize the LLF of the NLS-Weibull distribution.

Table 10: The MLE values of the fitted distributions for the DASE 3

Distributions	$\hat{\phi}_{MLE}$	$\hat{\delta}_{MLE}$	$\hat{\theta}_{MLE}$	$\hat{a}_{MLE}$	$\hat{b}_{MLE}$
NLS-Weibull	1.6944282	0.1748101	3.9686995	–	–
Weibull	–	0.0598919	5.7762681	–	–
K-Weibull	–	0.1302298	6.9052256	0.2176087	0.5679542
E-Weibull	0.68132852	0.0204663	7.2123305	–	–
NGL-Weibull	0.29350719	0.0718637	5.5546791	–	–
FRL-Weibull	21.2182143	0.2536367	4.4829746	–	–
NE-Weibull	–	0.0231207	6.5184216	–	–

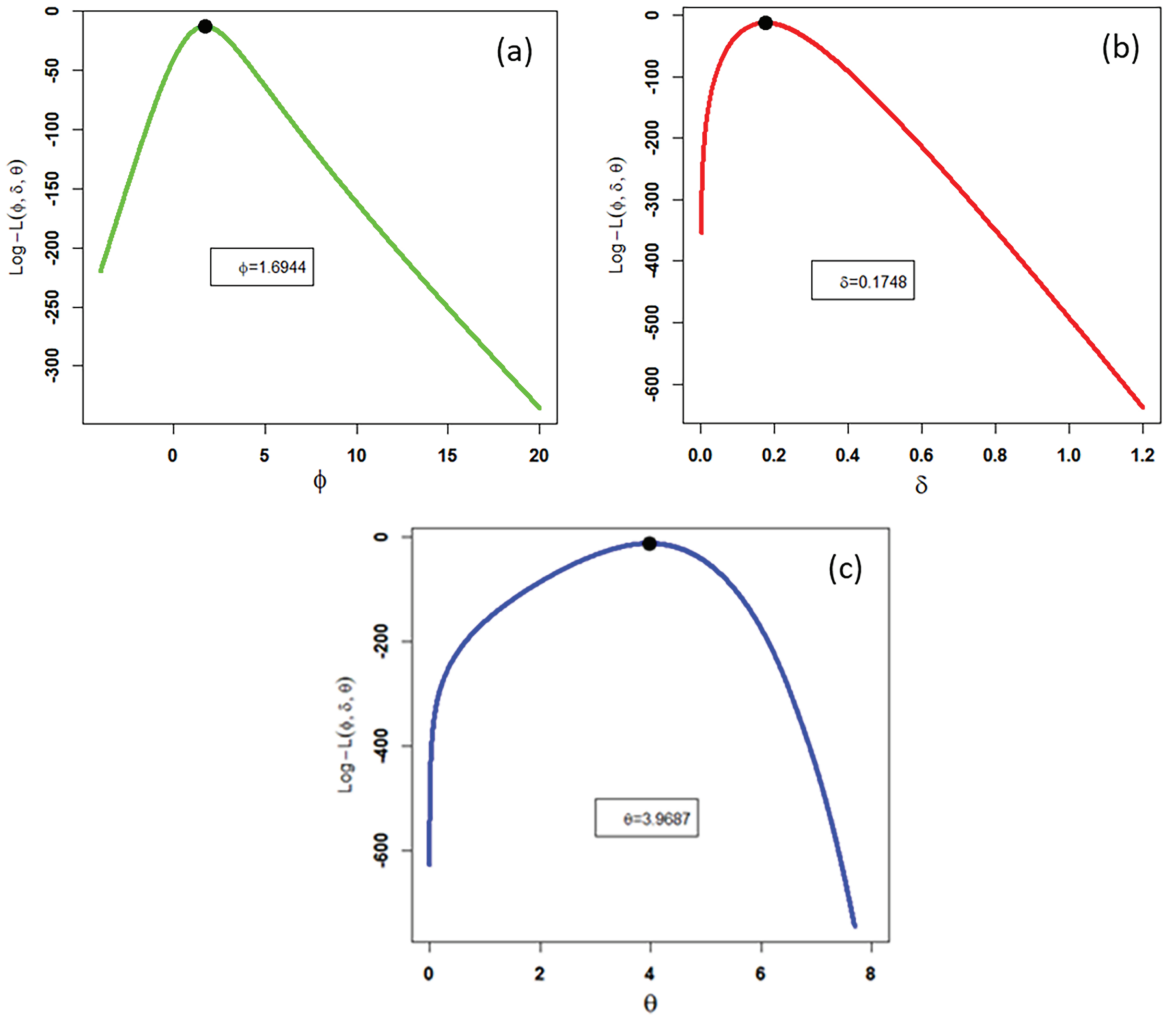

Figure 17: The profile log-likelihood plots of (**a**) $\hat{\phi}_{MLE}$, (**b**) $\hat{\delta}_{MLE}$, and (**c**) $\hat{\theta}_{MLE}$ of the NLS-Weibull distribution for DASE 3

Similarly, using DASE 3, the numerical values of the goodness of fit measures (i.e., GM_1, GM_2, and GM_3) and p-values of the fitted distributions are recorded in Table 11. Similarly, the numerical values of the discrimination measures (i.e., DM_1, DM_2, DM_3, and DM_4) are recorded in Table 12. Furthermore, to verify the flexibility and superiority of the NLS-Weibull distribution for the DASE 3, the fitted PDF plot, empirical CDF plot, fitted SF plot, and QQ plot are also visually illustrated in Fig. 17. Hence, from Tables 11 and 12, we can clearly see that all the GM_1, GM_2, GM_3, DM_1, DM_2, and DM_3 values of the NLS-Weibull distribution are smaller than those of the competing distributions. Besides, the p-value of the NLS-Weibull distribution is also higher than the competing distributions. Similarly, based on the graphical illustrations (i.e., Figs. 17 and 18), we can also see that the NLS-Weibull distribution has a close fit to the corresponding DASE 3.

Table 11: The goodness-of-fit criteria of the fitted distributions for DASE 3

Distributions	GM_1	GM_2	GM_3	p-values
NLS-Weibull	0.1401851	0.777564	0.12090	0.3158
Weibull	0.2373903	1.304515	0.15246	0.1069
K-Weibull	0.1674921	0.887547	0.17197	0.2225
E-Weibull	0.2010307	1.116805	0.14701	0.1313
NGL-Weibull	0.2372430	1.303132	0.15132	0.1117
FRL-Weibull	0.1558654	0.871452	0.14322	0.1508
NE-Weibull	0.2976632	1.630712	0.15695	0.0897

Table 12: The discrimination measures of the fitted distributions for DASE 3

Distributions	DM_1	DM_2	DM_3	DM_4
NLS-Weibull	31.77803	38.20743	32.18481	34.30674
Weibull	34.41374	39.70001	34.61374	36.09955
K-Weibull	35.46602	44.03856	36.15567	38.83764
E-Weibull	35.35289	41.78229	35.75967	37.88161
NGL-Weibull	36.37706	42.80647	36.78384	38.90578
FRL-Weibull	33.15126	39.58066	33.55804	35.67998
NE-Weibull	37.22426	41.51053	37.42426	38.91007

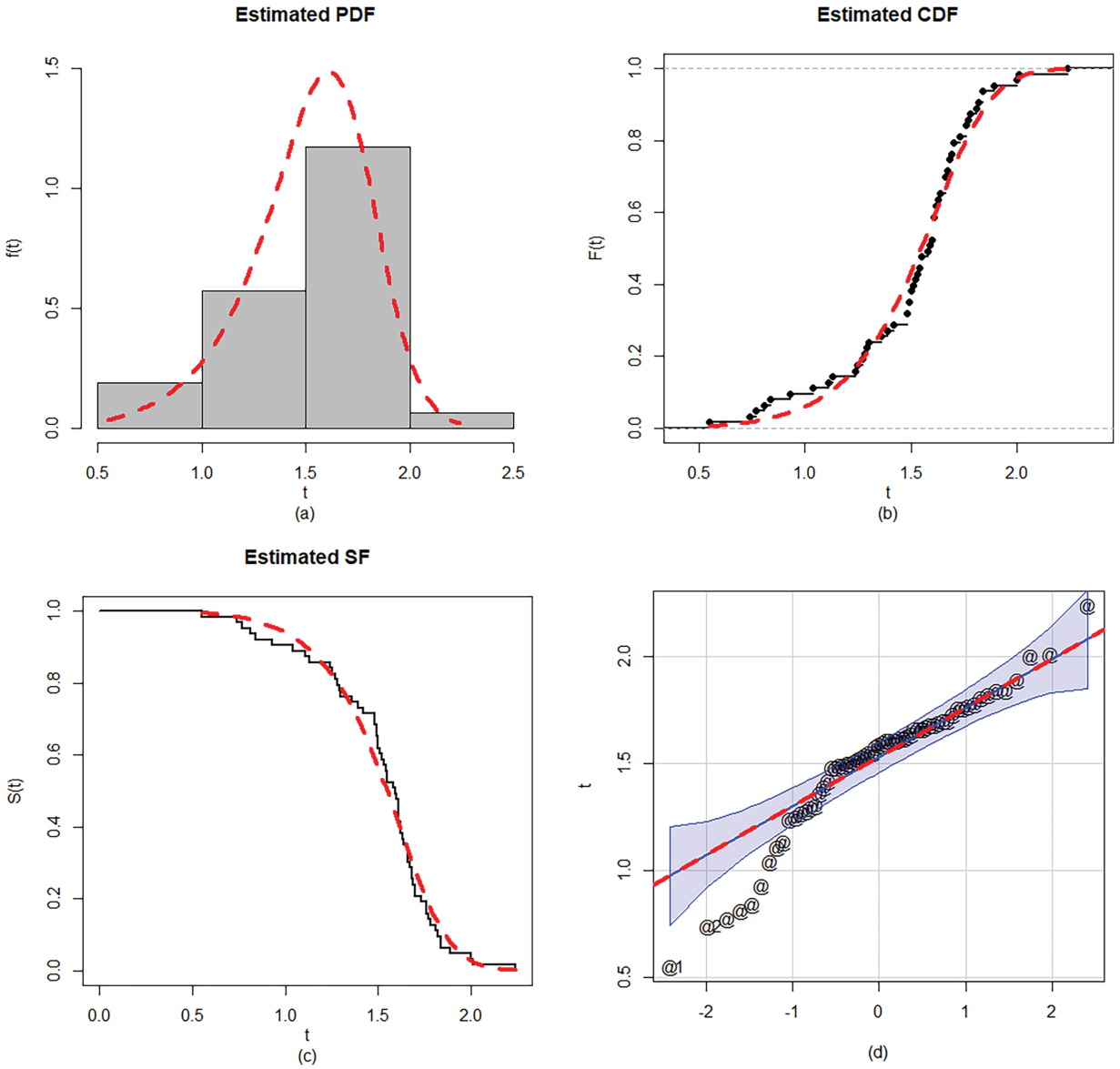

Figure 18: Visual illustration of the (**a**) estimated PDF plot, (**b**) estimated CDF plot, (**c**) estimated SF plot, and (**d**) Q-Q plot of the NLS-Weibull distribution using DASE 3

6.4 Illustrative Example Using Single Carbon Fibers DASE 4

Corresponding to DASE 3, some basic descriptive measures are: min. = 0.0312, 1st Qu. = 1.0980, median = 1.4780, mean = 1.4470, 3rd Qu. = 1.7730, max. = 2.5850, skewness = −0.1603059, kurtosis = 3.23563, variance = 0.2559907, and range = 2.5538. Furthermore, using DASE 4, the Box plot, Violin plot, and TTT-plot are sketched in Fig. 19.

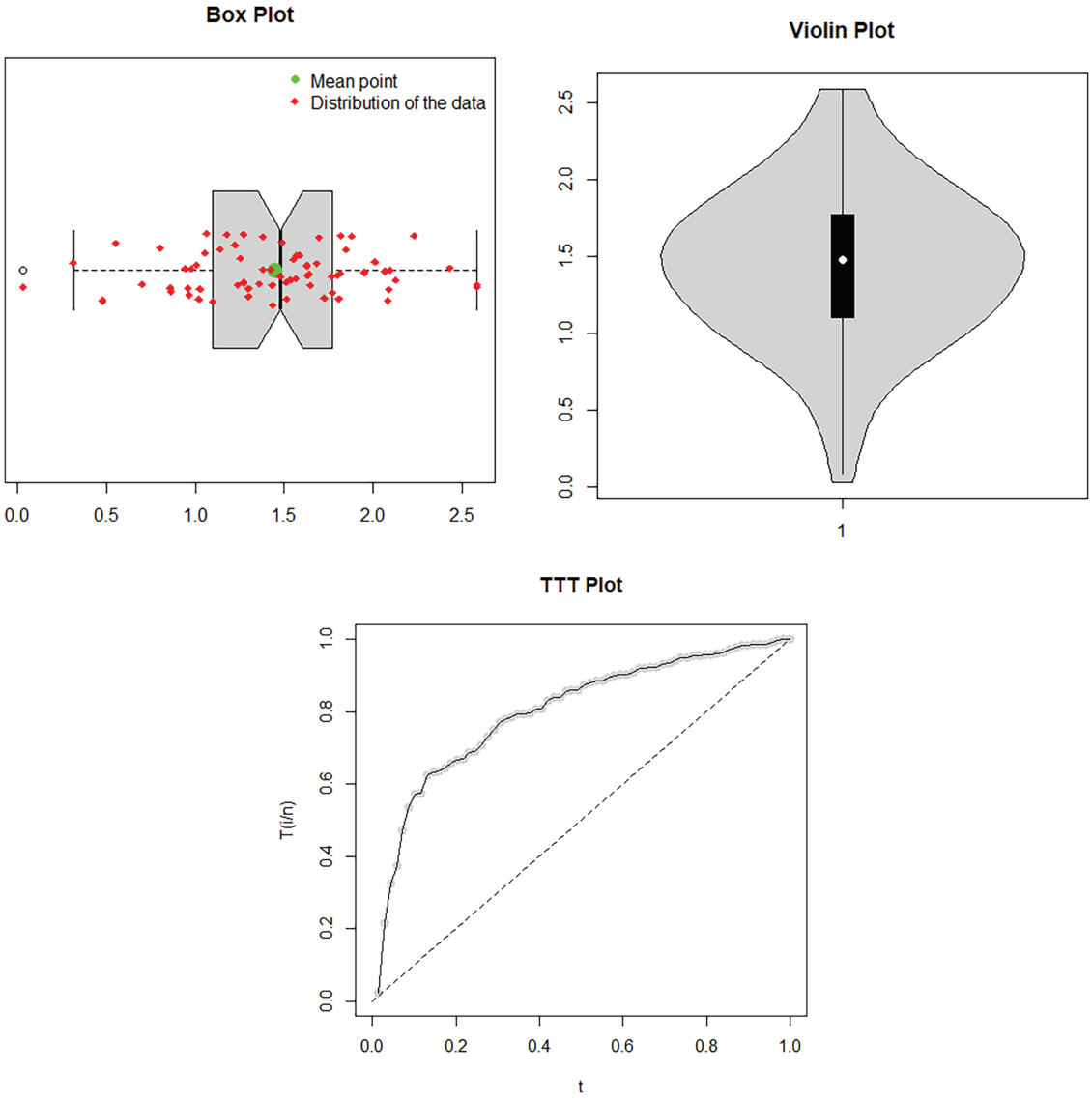

Figure 19: The Box, violin, and TTT plots for the DASE 4

Corresponding to DASE 4, the MLEs values (i.e., $\hat{\phi}_{MLE}$, $\hat{\delta}_{MLE}$, $\hat{\theta}_{MLE}$, $\hat{a}_{MLE}$, and $\hat{b}_{MLE}$) are recorded in Table 13. Moreover, for visual illustration, the profile log-likelihood function plots of each estimated parameter value of the NLS-Weibull distribution are plotted in Fig. 20. These profile log-likelihood plots demonstrated that the estimated values of the parameter for the considered data set are the unique root and local maximum because they maximize the LLF of the NLS-Weibull distribution.

Table 13: The MLE values of the fitted distributions for the DASE 4

Distributions	$\hat{\phi}_{MLE}$	$\hat{\delta}_{MLE}$	$\hat{\theta}_{MLE}$	$\hat{a}_{MLE}$	$\hat{b}_{MLE}$
NLS-Weibull	2.9095722	0.7750642	1.6704353	–	–
Weibull	–	0.2380486	3.0391581	–	–
K-Weibull	–	0.7250692	3.9482198	0.1642727	0.3984558
E-Weibull	0.5243200	0.0585258	4.5288845	–	–
NGL-Weibull	0.8598466	0.3363441	2.7185375	–	–
FRL-Weibull	19.1252681	0.7160035	2.3460322	–	–
NE-Weibull	–	0.1110387	3.4360919	–	–

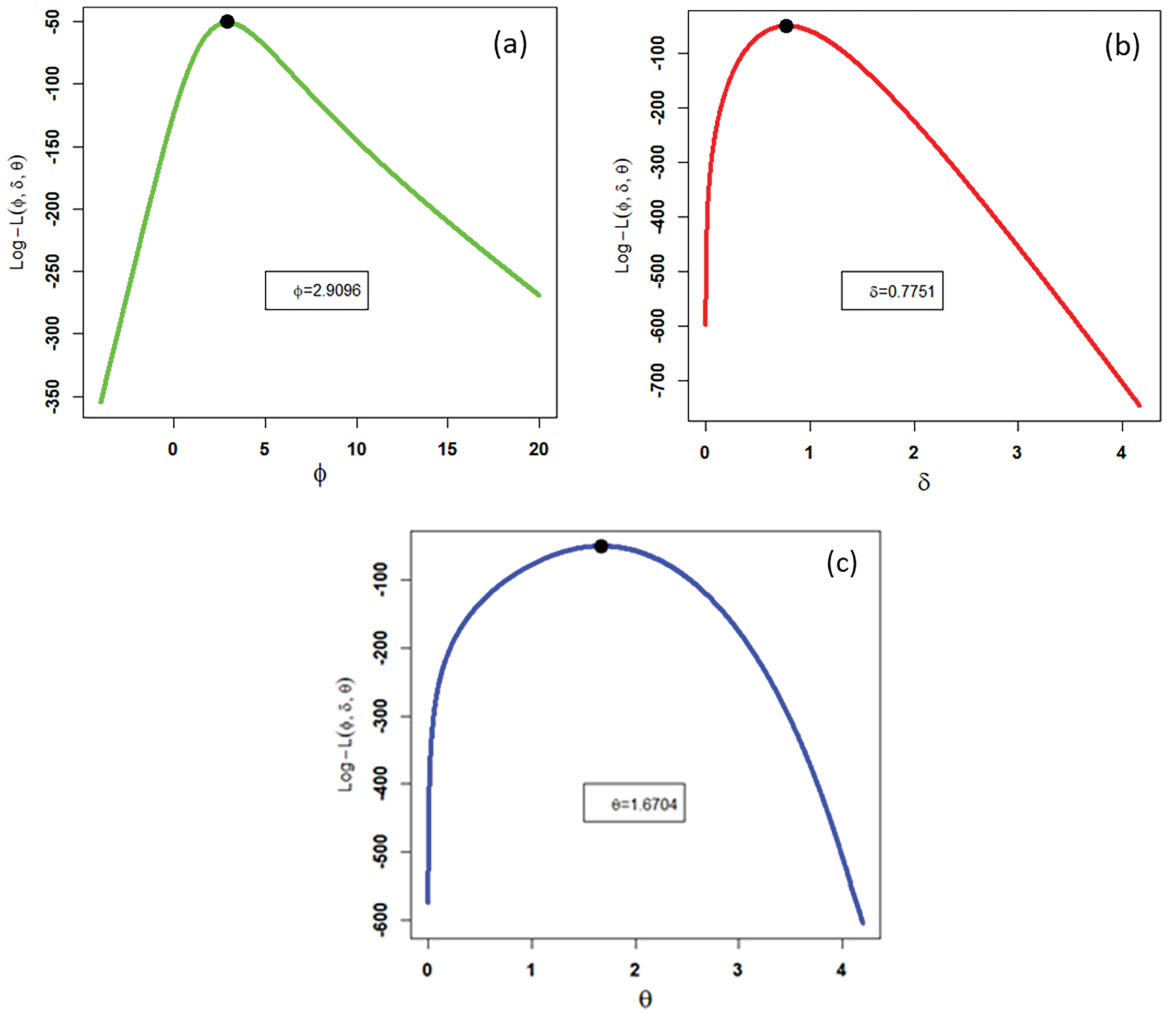

Figure 20: The profile log-likelihood plots of **(a)** $\hat{\phi}_{MLE}$, **(b)** $\hat{\delta}_{MLE}$, and **(c)** $\hat{\theta}_{MLE}$ of the NLS-Weibull distribution for DASE 4

Similarly, linked to DASE 4, the numerical values of the goodness of fit measures (i.e., GM_1, GM_2, and GM_3) and p-values of the fitted distributions are recorded in Table 14. Likewise, the numerical values of the discrimination measures (i.e., DM_1, DM_2, DM_3, and DM_4) are recorded in Table 15. Furthermore, to verify the flexibility and superiority of the NLS-Weibull distribution for the corresponding data set, the fitted PDF plot, empirical CDF plot, fitted SF plot, and QQ plot are also visually illustrated in Fig. 21. Hence, from Tables 14 and 15, we can obviously see that all the GM_1, GM_2, GM_3, DM_1, DM_2, and DM_3 values of the NLS-Weibull distribution are smaller as compared to the competing distributions. Besides, if we look at the p-values of the fitted distributions, the p-value of the NLS-Weibull distribution is also higher than the other competing distributions. Similarly, from Figs. 20 and 21, we can also see that the NLS-Weibull distribution has a close fit to the corresponding DASE 4. Consequently, from the above conversation and graphical illustration, it is concluded that the NLS-Weibull distribution suitable distribution (superior fit to the corresponding data) for the considered DASE 4 as compared to the competing distributions.

Table 14: The goodness of fit criteria of the fitted distributions for DASE 4

Distributions	GM_1	GM_2	GM_3	p-values
NLS-Weibull	0.0307930	0.2554147	0.048025	0.9973
Weibull	0.0830809	0.6075454	0.066105	0.9237
K-Weibull	0.0510924	0.4002251	0.072826	0.8577
E-Weibull	0.0710199	0.5364389	0.078662	0.7867
NGL-Weibull	0.0793725	0.5815207	0.062394	0.9510
FRL-Weibull	0.0616485	0.4739120	0.078324	0.7911
NE-Weibull	0.1126837	0.7887947	0.070369	0.8842

Table 15: The discrimination measures of the fitted distributions for DASE 4

Distributions	DM_1	DM_2	DM_3	DM_4
NLS-Weibull	107.4954	114.1977	107.8646	110.1544
Weibull	111.9152	116.3834	112.0971	113.6879
K-Weibull	110.4849	119.4204	111.1098	114.0294
E-Weibull	111.3913	118.0937	111.7606	114.0504
NGL-Weibull	113.6128	120.3151	113.9824	116.2718
FRL-Weibull	111.0795	117.7818	111.4487	113.7385
NE-Weibull	114.9838	119.4528	115.1656	116.7564

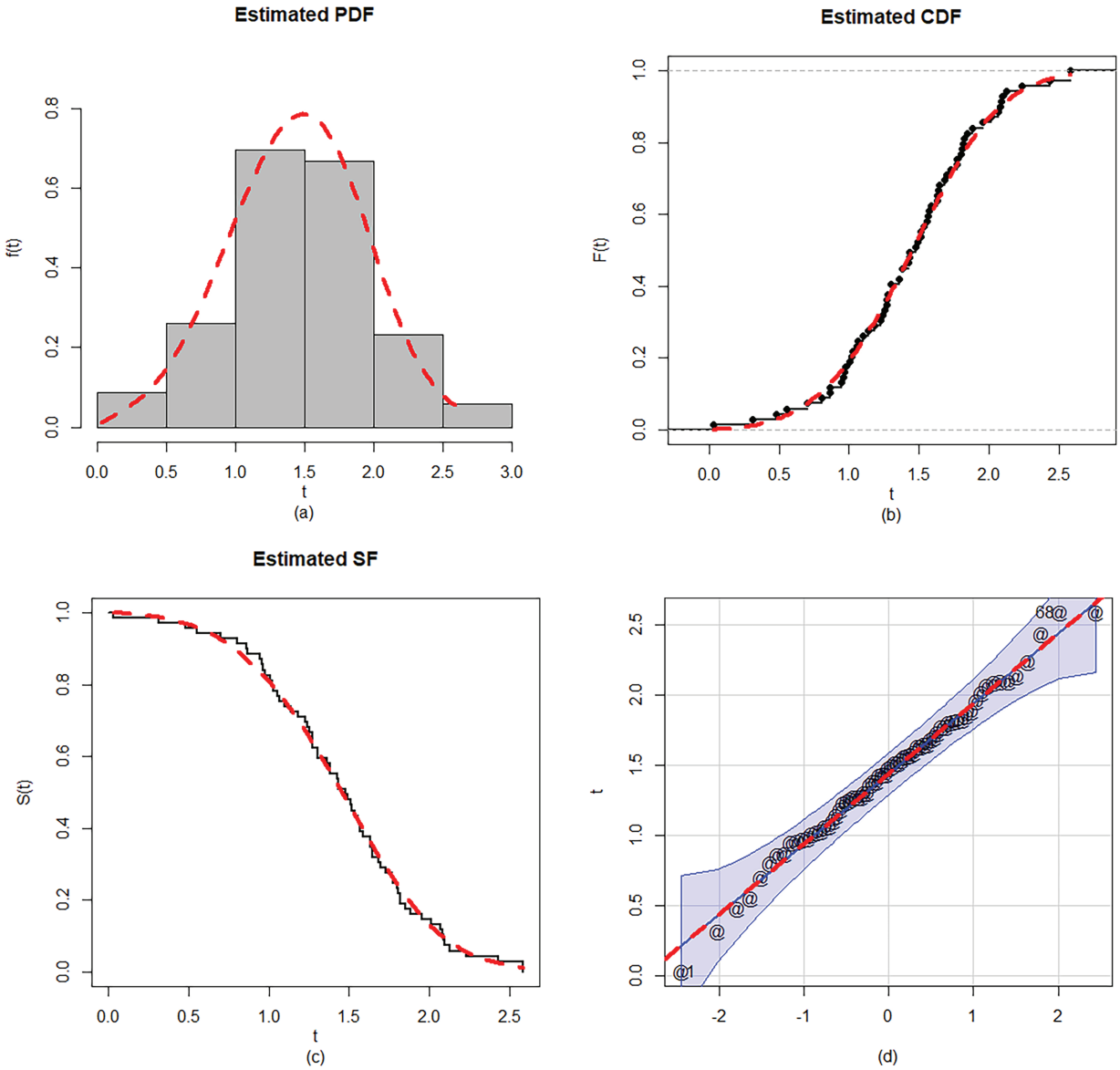

Figure 21: Visual illustration of the (**a**) estimated PDF plot, (**b**) estimated CDF plot, (**c**) estimated SF plot, and (**d**) Q-Q plot of the NLS-Weibull distribution using DASE 4

7 Summary

In this article, we incorporated logarithmic and trigonometric functions and developed a new family of distributions. The newly developed work is very attractive and is called the NLS-G family of distributions. The NLS-G family is developed by inserting one extra parameter to bring more flexibility to the classical distributions. For the developed work, some fundamental properties are examined. For estimating the model parameter of the NLS-G family, the well-known MLE method is employed. A Monte Carlo Simulation study is also conducted to evaluate the estimator's behaviors (estimated by the method of the MLE) of the proposed work. Based on the NLS-G family, a new extension

of the Weibull distribution is made. The new extension is called the NLS-Weibull distribution. The CDF and SF of the NLS-Weibull distribution are sketched graphically. Furthermore, the PDF and HF of the NLS-Weibull distribution are also sketched graphically. The PDF graphs of the NLS-Weibull distribution are left-skewed, symmetrical, and right-skewed. Similarly, the HF graphs of the NLS-Weibull distribution are increasing, decreasing, unimodal, increasing-decreasing-increasing, and bathtub shapes. The HF graphs of the NLS-Weibull distribution make this proposed family of distributions suitable/applicable for modeling data with both monotone and non-monotone hazard rate functions. Finally, four data sets from the field of the engineering sector are taken for comparison purposes of the NLS-Weibull distribution in comparison with existing distributions. Four model adequacy measures (diagnostic measures) are investigated for comparison purposes to compare the numerical results of the proposed distribution with other competing distributions. Based on these model adequacy measures and other graphical illustrations, it is concluded that the NLS-Weibull distribution provided the best fit compared to the competing distributions. We hope that this novel approach to distributions will inspire researchers to use their findings in the engineering sciences and other disciplines.

Acknowledgement: The authors extend their appreciation to Taif University, Saudi Arabia, for supporting this work.

Funding Statement: This research was funded by Taif University, Saudi Arabia, Project No. (TU-DSPP-2025-39).

Author Contributions: The authors confirm contribution to the paper as follows: Conceptualization, Zubir Shah and Dost Muhammad Khan; Methodology, Zubir Shah and Dost Muhammad Khan; Software, Zubir Shah; Validation, Amirah Saeed Alharthi; Formal Analysis, Zubir Shah and Dost Muhammad Khan; Investigation, Amirah Saeed Alharthi; Resources, Amirah Saeed Alharthi and Hassan M. Aljohani; Data Curation, Amirah Saeed Alharthi and Hassan M. Aljohani; Writing—Original Draft, Zubir Shah; Writing—Review & Editing, Dost Muhammad Khan and Amirah Saeed Alharthi; Visualization, Amirah Saeed Alharthi and Hassan M. Aljohani; Supervision, Dost Muhammad Khan; Project Administration, Dost Muhammad Khan; Funding Acquisition, Amirah Saeed Alharthi and Hassan M. Aljohani. All authors reviewed and approved the final version of the manuscript.

Availability of Data and Materials: The data that support the findings of this study are available from the corresponding author, upon reasonable request.

Ethics Approval: Not applicable.

Conflicts of Interest: The authors declare no conflicts of interest.

References

1. Almalki SJ, Yuan J. A new modified Weibull distribution. Reliab Eng Syst Saf. 2013;111(1):164–70. doi:10.1016/j.ress.2012.10.018.
2. Mudholkar GS, Srivastava DK. Exponentiated Weibull family for analyzing bathtub failure-rate data. IEEE Trans Reliab. 1993;42(2):299–302. doi:10.1109/24.229504.
3. Nadarajah S, Kotz S. The exponentiated Fréchet distribution. Interstat Electron J. 2003;14:1–7.

4. Nadarajah S. The exponentiated exponential distribution: a survey. Asta Adv Stat Anal. 2011;95(3):219–51. doi:10.1007/s10182-011-0154-5.
5. Salem HM. The exponentiated *Lomax* distribution: different estimation methods. Am J Appl Math Stat. 2014;2(6):364–8. doi:10.12691/ajams-2-6-2.
6. Ashour SK, Eltehiwy MA. Exponentiated power Lindley distribution. J Adv Res. 2015;6(6):895–905. doi:10.1016/j.jare.2014.08.005.
7. Marshall AW, Olkin I. A new method for adding a parameter to a family of distributions with application to the exponential and Weibull families. Biometrika. 1997;84(3):641–52. doi:10.1093/biomet/84.3.641.
8. Ghitany ME, Al-Hussaini EK, Al-Jarallah RA. Marshall-Olkin extended weibull distribution and its application to censored data. J Appl Stat. 2005;32(10):1025–34. doi:10.1080/02664760500165008.
9. Ghitany ME, Al-Awadhi FA, Alkhalfan LA. Marshall-olkin extended *Lomax* distribution and its application to censored data. Commun Stat Theory Meth. 2007;36(10):1855–66. doi:10.1080/03610920601126571.
10. Krishna E, Jose KK, Alice T, Ristić MM. The Marshall-olkin Fréchet distribution. Commun Stat Theory Meth. 2013;42(22):4091–107. doi:10.1080/03610926.2011.648785.
11. Al-Saiari AY, Baharith LA, Mousa SA. Marshall-olkin extended burr type XII distribution. Int J Stat Probab. 2013;3(1):78–84. doi:10.5539/ijsp.v3n1p78.
12. Mahdavi A, Kundu D. A new method for generating distributions with an application to exponential distribution. Commun Stat Theory Meth. 2017;46(13):6543–57. doi:10.1080/03610926.2015.1130839.
13. Dey S, Sharma VK, Mesfioui M. A new extension of weibull distribution with application to lifetime data. Ann Data Sci. 2017;4(1):31–61. doi:10.1007/s40745-016-0094-8.
14. Ihtisham S, Khalil A, Manzoor S, Ahmad Khan S, Ali A. Alpha-Power Pareto distribution: its properties and applications. PLoS One. 2019;14(6):e0218027. doi:10.1371/journal.pone.0218027.
15. Dey S, Ghosh I, Kumar D. Alpha-power transformed Lindley distribution: properties and associated inference with application to earthquake data. Ann Data Sci. 2019;6(4):623–50. doi:10.1007/s40745-018-0163-2.
16. Amer YM. Alpha-power transformed *Lomax* distribution: properties and application. J Appl Sci Res. 2020;16(3):7–20.
17. ZeinEldin RA, Ahsan ul Haq M, Hashmi S, Elsehety M. Alpha power transformed inverse *Lomax* distribution with different methods of estimation and applications. Complexity. 2020;2020(1):1860813. doi:10.1155/2020/1860813.
18. Bakr ME, Al-Babtain AA, Mahmood Z, Aldallal RA, Khosa SK, Abd El-Raouf MM, et al. Statistical modelling for a new family of generalized distributions with real data applications. Math Biosci Eng. 2022;19(9):8705–40. doi:10.3934/mbe.2022404.
19. Alsadat N, Ahmad A, Jallal M, Gemeay AM, Meraou MA, Hussam E, et al. The novel Kumaraswamy power Frechet distribution with data analysis related to diverse scientific areas. Alex Eng J. 2023;70:651–64. doi:10.1016/j.aej.2023.03.003.
20. Shah Z, Khan DM, Khan I, Hussain S, Alghamdi FM, Aljohani HM. A new flexible odd type-G family of distributions with properties and applications in the biomedical sector. Sci Rep. 2025;15(1):35490. doi:10.1038/s41598-025-19351-6.
21. Osi A, Singh Raghav Y, Ahmad Sabo S, Zakariyya Musa I. The new transformed Sine G family of distribution with inferences and application. Braz J Biom. 2025;43(3):1–15. doi:10.28951/bjb.v43i3.755.
22. Hassan AS, Alsadat N, Elgarhy M, Sapkota LP, Balogun OS, Gemeay AM, et al. A novel asymmetric form of the power half-logistic distribution with statistical inference and real data analysis. Era. 2025;33(2):791–825. doi:10.3934/era.2025036.
23. Alsolmi MM. A new logarithmic tangent-U family of distributions with reliability analysis in engineering data. Comput J Math Stat Sci. 2025;4(1):258–82. doi:10.21608/cjmss.2025.342223.1090.

24. Zhao Y, Ahmad Z, Alrumayh A, Yusuf M, Aldallal R, Elshenawy A, et al. A novel logarithmic approach to generate new probability distributions for data modeling in the engineering sector. Alex Eng J. 2023;62(1):313–25. doi:10.1016/j.aej.2022.07.021.
25. Shah Z, Khan DM, Khan Z, Faiz N, Hussain S, Anwar A, et al. A new generalized logarithmic-X family of distributions with biomedical data analysis. Appl Sci. 2023;13(6):3668. doi:10.3390/app13063668.
26. Alzaatreh A, Lee C, Famoye F. A new method for generating families of continuous distributions. METRON. 2013;71(1):63–79. doi:10.1007/s40300-013-0007-y.
27. Kamal M, Rao GS, Alsolmi MM, Ahmad Z, Aldallal R, Rahman MM. A new statistical methodology using the sine function: control chart with an application to survival times data. PLoS One. 2023;18(8):e0285914. doi:10.1371/journal.pone.0285914.
28. Chamunorwa S, Makubate B, Oluyede B, Chipepa F. The exponentiated half logistic-log-logistic Weibull distribution: model, properties and applications. J Stat Model Theory Appl. 2021;2(1):101–20.
29. Alnssyan B, Ahmad Z, Malela-Majika JC, Seong JT, Shafik W. On the identifiability and statistical features of a new distributional approach with reliability applications. AIP Adv. 2023;13(12):125211. doi:10.1063/5.0178555.
30. Nagarjuna VBV, Vardhan RV, Chesneau C. Kumaraswamy generalized power *Lomax* distributionand its applications. Stats. 2021;4(1):28–45. doi:10.3390/stats4010003.
31. Cordeiro GM, Ortega EMM, Nadarajah S. The Kumaraswamy Weibull distribution with application to failure data. J Frankl Inst. 2010;347(8):1399–429. doi:10.1016/j.jfranklin.2010.06.010.
32. Weibull W. A statistical distribution function of wide applicability. J Appl Mech. 1951;18(3):293–7. doi:10.1115/1.4010337.
33. Shah Z, Ali A, Hamraz M, Khan DM, Khan Z, EL-Morshedy M, et al. A new member of T-X family with applications in different sectors. J Math. 2022;2022(1):1453451. doi:10.1155/2022/1453451.
34. Liu Y, Ilyas M, Khosa SK, Muhmoudi E, Ahmad Z, Khan DM, et al. A flexible reduced logarithmic-X family of distributions with biomedical analysis. Comput Math Methods Med. 2020;2020(3):4373595. doi:10.1155/2020/4373595.